AD-A131 618 FUNDAMENTAL RESEARCH DIRECTED TO ADVANCED HIGH TEMPERATURE COATING SYSTEM..(U) PITTSBURGH UNIV PA DEPT OF METALLURGICAL AND MATERIALS ENGINE.. 1/1

UNCLASSIFIED G H MEIER ET AL. 07 JUN 83 AFOSR-TR-83-0723 F/G 11/3 NL

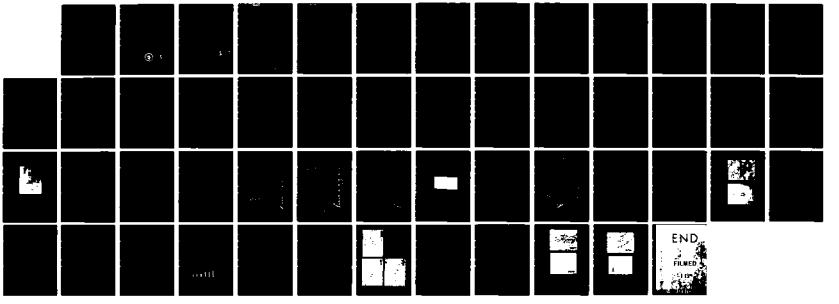

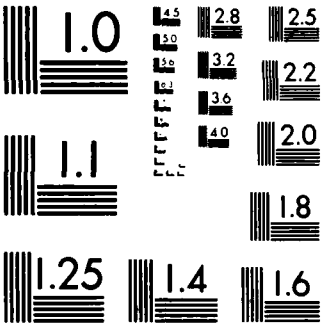

FUNDAMENTAL RESEARCH DIRECTED
TO ADVANCED HIGH TEMPERATURE
COATING SYSTEMS BEYOND THE
CURRENT STATE-OF-THE-ART SYSTEMS

METALLURGICAL AND MATERIALS ENGINEERING

University of Pittsburgh
Pittsburgh, Pennsylvania 15261

FUNDAMENTAL RESEARCH DIRECTED TO ADVANCED HIGH TEMPERATURE COATING SYSTEMS BEYOND THE CURRENT STATE-OF-THE-ART SYSTEMS

by

G. H. Meier

and

F. S. Pettit

Metallurgical and Materials Engineering Department
University of Pittsburgh
848 Benedum Hall
Pittsburgh, PA 15261

Report Period

January 1, 1982 - December 31, 1983

SECURITY CLASSIFICATION OF THIS PAGE (When Data Entered)

UNCLASSIFIED

REPORT DOCUMENTATION PAGE

READ INSTRUCTIONS BEFORE COMPLETING FORM

1. REPORT NUMBER: AFOSR-TR- 83-0723	2. GOVT ACCESSION NO.: AD-A131 618
3. RECIPIENT'S CATALOG NUMBER:	
4. TITLE (and Subtitle): Fundamental Research Directed to Advanced High Temperature Coating Systems Beyond the Current State of the Art Systems.	5. TYPE OF REPORT & PERIOD COVERED: Third Annual Report January 1-December 31, 1982
	6. PERFORMING ORG. REPORT NUMBER:
7. AUTHOR(s): G. H. Meier and F. S. Pettit	8. CONTRACT OR GRANT NUMBER(s): AFOSR-80-0089
9. PERFORMING ORGANIZATION NAME AND ADDRESS: Department of Metallurgical/Materials Engineering University of Pittsburgh 848 Benedum Hall, Pittsburgh, PA 15261	10. PROGRAM ELEMENT, PROJECT, TASK AREA & WORK UNIT NUMBERS: 61102F 2306/A2
11. CONTROLLING OFFICE NAME AND ADDRESS: Electronic and Materials Science Air Force Office of Scientific Research Bolling Air Force Base, DC 20332	12. REPORT DATE: June 7, 1983
	13. NUMBER OF PAGES: 46
14. MONITORING AGENCY NAME & ADDRESS(if different from Controlling Office)	15. SECURITY CLASS. (of this report): UNCLASSIFIED
	15a. DECLASSIFICATION/DOWNGRADING SCHEDULE

16. DISTRIBUTION STATEMENT (of this Report)

Approved for public release, distribution unlimited.

17. DISTRIBUTION STATEMENT (of the abstract entered in Block 20, if different from Report)

18. SUPPLEMENTARY NOTES

19. KEY WORDS (Continue on reverse side if necessary and identify by block number)

Oxidation, oxide scale adherence, coatings.

20. ABSTRACT (Continue on reverse side if necessary and identify by block number)

The oxidation in air of nickel-silicon alloys with compositions extending from 5 to 20 weight-silicon have been studied over the temperature interval between 900° and 1100°C. In the case of alloys with less than 20% silicon, the silicon is not oxidized internally nevertheless the rates of oxidation are greater than those for alloys upon which alumina scales are formed. The alloy with 20% silicon exhibited oxidation rates less than those associated with alumina scales under similar conditions. The scales which developed upon the Ni-20 silicon alloy are in the process of being identified. It appears that silicon rich coatings have the

DD FORM 1 JAN 73 1473 EDITION OF 1 NOV 65 IS OBSOLETE

UNCLASSIFIED

SECURITY CLASSIFICATION OF THIS PAGE (When Data Entered)

potential of being used in place of present state-of-the-art MCrAlY coatings.

The adherence of alumina formed on alloys of Ni-20Cr-10Al and Co-20Cr-10Al with yttrium or hafnium has been studied by using cyclic oxidation tests, acoustic emission measurements and by measuring the load required to pull scales from substrates. These studies have shown that the following parameters affect alumina scale adherence:

-oxygen active element type and concentration
-base alloy composition (e.g. nickel-versus cobalt-base)
-alloy surface condition
-specimen cooling rate
-exposure time of specimen to oxidation conditions.

The acoustic emission technique of studying damage in alumina scales on alloys appears to provide a means of nondestructively determining the useful lives of coatings on alloys that remain after use under service conditions.

TABLE OF CONTENTS

INTRODUCTION

The objective of this program is to define coatings compositions, structures and surface treatments that may be used to develop advanced metallic coatings possessing superior high temperature oxidation resistance compared to the current state-of-the-art MCrAlY systems and diffusion aluminide coatings. The approach which has been used to develop high temperature oxidation resistance in coatings has consisted of using reaction product barriers to separate the reactants (i.e. the alloy and the environment) and thereby inhibit the rate of degradation. An approach better than this traditional one has not been devised and consequently the current program was concerned with determining what reaction products were the best barriers in minimizing degradation, and how some of the more protective barriers could be made even more effective.

A number of oxide systems were examined in this program to determine if they could be used to develop high temperature oxidation resistance in alloys via selective oxidation. Alpha - Al_2O_3 and a silicon-rich oxide were the only systems which exhibited growth rates slow enough to provide adequate protection against oxidation at temperatures above 1000°C for extended periods of time. These results showed that, if the use of diffusion barriers or inhibitors between alloys and coatings was excluded*, two approaches could be used to attempt to obtain more advanced high temperature systmes. One approach should involve the use of silicon-containing scales as protective barriers to inhibit oxidation. The other should attempt to optimize α-Al_2O_3

*Such approaches were excluded as not within the scope of this program as opposed to not being feasible approaches.

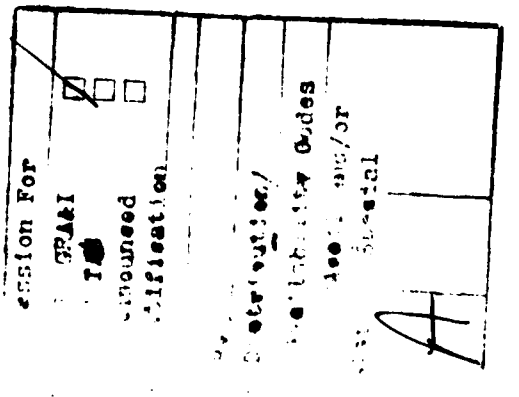

scale adhesion, reforming capability, and structure through alloy surface structure and composition.

A number of nickel-silicon alloys were studied in this program. Most of these alloys exhibited significant amounts of transient oxidation but eventually steady state oxidation rates were observed similar to those for the Al_2O_3 - forming systems. This slow steady-state oxidation was ascribed to the formation of a sealing layer of SiO_2 at the alloy - scale interface. This oxide barrier appeared to be slightly permeable to nickel which resulted in continued formation of NiO at the scale-gas interface. Exposure of alloys to gases with reduced oxygen pressure ($P_{O_2} \sim 10^{-5}$ atm) resulted in a thin scale which appeared to be impermeable to nickel. No detrimental effects of low P_{O_2} due to SiO evaporation were observed. These results suggested that more protective silicon-containing scales may be obtained through appropriate control of alloy composition. In subsequent sections of this report the results obtained during the third year of this program from additional studies of the oxidation of nickel-silicon alloys are presented.

The studies performed with the Al_2O_3- formers involved the use of NiCrAl and CoCrAl alloys and these alloys with small additions of yttrium or hafnium. During the course of these studies it became obvious that in order to compare oxide scale adhesion on the different alloys other techniques in addition to cyclic oxidation measurements had to be used. Experiments were conducted on quantitatively assessing and comparing scale adherence by measuring the stress required to pull oxide scales from substrates. Also, the possibility of using acoustic emission to study in situ the cracking and spalling of oxide scales was examined and found to be promising. Finally the data that were generated on the Al_2O_3 scales indicated that the adherence of α-Al_2O_3 scales on alloys can vary and depends upon a number of factors

which includes alloy surface condition and oxygen active element type and concentration. In subsequent sections of this report results are presented that have been obtained during the third year of this program for the efforts concerned with Al_2O_3 scales. This work consisted of more extensive studies of the acoustic emission technique to examine Al_2O_3 protectiveness and more detailed analyses of the factors which critically affect oxide scale adherence.

EXPERIMENTAL APPROACH

The experimental techniques used in this study involved the more or less traditional methods for studying high temperature oxidation with one important exception. An acoustic emission technique was used to attempt to define cracking in the Al_2O_3 scales. In the following the traditional techniques will be discussed briefly and then the studies involving acoustic emission will be discussed in somewhat more detail.

Specimen Preparation

Alloys were prepared by tungsten arc melting under an argon atmosphere and drop casting into molds. The dimensions of the molds were 150 mm X 25 mm X 9 mm or 150 mm X 16 mm dia. The ingots were homogenized by heating in argon for 100 hrs. at 1150°C. Specimen shapes were either 12 mm X 9 mm X 2 mm or 16 mm dia. X 2 mm. The specimens were polished through 600 grit and ultrasonically cleaned in alcohol prior to oxidation testing.

Isothermal Oxidation

Isothermal oxidation testing was performed by using a Cahn Microbalance and a furnace assembly consisting of a quartz reaction tube and appropriate glassware to provide a gas tight system. The specimens were oxidized in flowing or static air and weight changes were measured continuously as a function of time.

Cyclic Oxidation

Long term cyclic oxidation testing was carried out by exposing specimens in laboratory air in an apparatus which automatically removed the specimens from the furnace and reinserted them at selected time intervals. Each cycle consisted of 45 minutes isothermal oxidation followed by cooling for 15 minutes outside the furnace. The specimens were weighed every 20 to 30 hours exposure time.

Examination of Exposed Specimens

Specimens were examined routinely by using optical metallography, scanning electron microscopy and x-ray diffraction. Some specimens were occasionally examined by using scanning auger microscopy.

Acoustic Emission Experiments

An apparatus was constructed in order to use acoustic emission as a means of describing oxide scale cracking on the surfaces of alloys, Figure 1.

Acoustic emission studies are usually carried out by attaching a piezoelectric transducer to the specimen. The transducer detects the acoustic signal (elastic wave) and transforms it into an electric signal. However, no transducer is available which can withstand the high temperatures of interest in the current study. Therefore, a wave guide was used to transmit the acoustic signal from the specimen hanging inside the furnace to the transducer position outside, as shown schematically in Figure 2. The wave guide was a 1 mm diameter platinum rod 1m in length which had one end spot-welded to the specimen and the other attached to a stainless steel cone to which the transducer was attached. Platinum was chosen since it does not oxidize under the experimental conditions used and does not undergo any phase transformations in the temperature range of interest. An alumina wave guide was also developed but has not been used in the present study as yet.

The acoustic emission apparatus used was a Dunegan-Endevco--3000 series acoustic emission detection system. Figure 3 is a function block diagram of the apparatus. The acoustic signal from the specimen is transmitted through the waveguide and transformed into an electrical signal by the transducer. This signal is preamplified and filtered before passing into a secondary amplifier. The amplified and filtered signal is then fed into a counter which counts the number of times the signal exceeds the threshold level (1 volt) for triggering the counter. The signal, shown schematically in Figure 4, consists of a damped sinusoidal wave with a frequency corresponding approximately to the resonant frequency of the transducer. A given acoustic emission event within the specimen produces several counts associated with the number of times the signal crosses the threshold voltage, Vt, in "ringing down" to a voltage below the trigger level. Three counts would result from the signal shown in Figure 4. Larger events produce more counts in ringing down so the number of counts is a measure of the energy released in an event.

All specimens were usually oxidized for 24 hours in air at 1000, 1050, or 1100°C and then cooled either in the furnace or outside in the air. The specimen temperature as a function of time was obtained from a thermocouple welded to a dummy specimen. Acoustic emission counts were recorded both during isothermal oxidation and the cooling periods. However, during cooling a total signal amplification of 80 dB was used while during isothermal oxidation a 90 dB gain was used since the acoustic emission activity was weak during the latter.

RESULTS AND DISCUSSION

In this section the results obtained from the oxidation of nickel-silicon alloys will be discussed first and then results obtained from the studies of alumina scales on MCrAl and MCrAlY alloys will be presented.

Oxidation of Nickel-Silicon Alloys

The phase diagram for the nickel-silicon system[1] is presented in Figure 5. Nickel-silicon alloys with the compositions presented in Table I were prepared by casting. After homogenization these alloys were examined by using optical metallography and the phases present were compared with the phase diagram. Tentative agreement between the phase diagram and the observed phases was obtained.

All of the alloys were polished and oxidized isothermally in air at temperatures of 900°, 1000° and 1100°C. The weight change versus time curves for these alloys are presented in Figures 6,7 and 8*. It can be seen for all of the alloys that the weight change versus time curves exhibited less oxidation (as indicated by the magnitude of the weight changes) as the silicon content was increased.

Visual examination of the specimens after oxidation showed that the oxidation products had formed nonuniformly over the specimen surfaces. In some areas a substantial amount of a green-colored oxide was evident whereas in other areas the oxide was colorless and transparent. X-ray diffraction analysis showed that both NiO and SiO_2 had been formed. On the low silicon alloys the green oxide was most abundant and it became less apparent as the silicon content was increased. It has not been detected on the Ni-20Si alloy. On those alloys where NiO was observed, internal oxidation of the silicon

*Porosity in the Ni-15Si may have caused the Ni-15Si alloy to exhibit oxidation rates similar to the Ni-5Si alloy. Another alloy with the composition Ni-15Si is being prepared. No data on the Ni-15Si alloy with porosity will be presented in this report.

was not evident, Figure 9. These results indicate that silicon is not being oxidized internally but is diffusing to the surfaces of the alloys where it is being oxidized and incorporated into the external oxide scale.

The weight change versus time curves for all of the alloys did not conform to a parabolic rate law. These oxidation rates were slower than parabolic. The weight change versus time data as well as the metallographic results indicate that all of the alloys which have been studied undergo a period of transient oxidation whereby the amount of silicon in the scale is progressively increasing. Hence the oxidation rates are less than parabolic because the proportions of nickel and silicon in the external scales formed on the alloys are changing with time. In view of this condition it is expected that the oxidation of all of the alloys should eventually be controlled by diffusion through the silicon enriched scales. The results currently available, however, indicate that only alloys with at least 20% silicon form continuous scales of silica. Work is being directed towards attempting to account for this apparent lack of development of continuous silica scales on those alloys containing less than 20% silicon even though no internal oxidation of the silicon has been observed.

The nickel-silicon alloys containing at least 20% silicon have been found to exhibit extremely slow rates of oxidation. The weight changes versus time for a Ni-20Si alloy and a CoCrAlY alloy upon which an αAl_2O_3 scale is formed are compared in Figure 10. It can be seen that the weight changes for the Ni-20Si alloy are significantly less than those for the CoCrAlY alloy. These results indicate that silicide coatings should be considered further in regards to their use as replacements of alumina-forming coatings.

Work is continuing to examine the oxidation behavior of the Ni-20Si and alloys with higher silicon concentrations. Preliminary cyclic oxidation data

are presented in Figure 11. As can be seen in this Figure virtually no oxide cracking or spalling was observed for Ni-20Si. Examination of this specimen from the cyclic oxidation test showed that an extremely thin, transparent oxide scale had been formed. Such results strongly support the argument that silica scales may provide improved oxidation resistance in comparison to alumina-forming alloys.

Alumina Formation and Adherence on NiCrAl and CoCrAl Alloys

As described in the second annual report for this program[2], it had been observed that surface conditions and ion implantation affected alumina scale adherence and reforming capability, however, definition of the critical parameters which were responsible for these observed results were difficult to identify precisely via cyclic oxidation testing. Hence, during the third year of this program emphasis was placed on developing test methods that could be used along with cyclic oxidation tests to more effectively describe the effects of oxygen active elements on alumina scale adhesion, cracking and spalling. These studies were concerned with alumina formation and adherence and involved the use of the alloys whose compositions are presented in Table II.

Experiments were performed to compare acoustic emission counts on alloys upon which adherent and nonadherent α-Al_2O_3 scales were formed during oxidation. Specimens of CoCrAl (A) and CoCrAlY (B) were oxidized 24 hours at 1050°C and the acoustic emission counts detected during cooling are presented in Figures 12 and 13. Inspection of these two Figures shows two significant differences. First the total counts recorded for the CoCrAl alloy was about two orders of magnitude greater than for the CoCrAlY alloy. Such results, indicating more damage to the oxide formed on the CoCrAl specimen, were consistent with the appearance of the specimen surfaces, Figure 14, where the scale had spalled

much more severely from the CoCrAl specimen compared to the CoCrAlY specimen. The second difference in the data involved the temperature at which damage was first detected in the oxide scales. This temperature was 700°C for the CoCrAl specimen compared to 400°C for the CoCrAlY specimen. These results clearly show that acoustic emission can be used to differentiate between the cracking and spalling of alumina from CoCrAl and CoCrAlY alloys. More importantly, the observation that cracking and spalling upon cooling occurs on CoCrAl before CoCrAlY shows that adherence of the alumina to the CoCrAlY substrate is greater than to the CoCrAl substrate, or that larger stresses are generated on cooling in the alumina on the CoCrAl substrate compared to the alumina on the CoCrAlY substrate.

In a second set of experiments the relative effectiveness of yttrium and hafnium additions on the scale adherence and cyclic oxidation behavior of NiCrAl and CoCrAl alloys was investigated. Alloys D (NiCrAlY), F (NiCrAlHf), H(CoCrAlY), and J(CoCrAlHf) were each oxidized for 24 hours in air and air cooled outside the furnace. The AE counts measured during cooling for these alloys are presented in Figure 15. It is clear that the acoustic emission counts are orders of magnitude less than for an alloy with no oxygen-active element (for example CoCrAl in Fig. 12). However, there are significant differences among the alloys. There is relatively little difference between the two Co-base alloys but both exhibit far less acoustic emission than the Ni-base alloys. In addition, Hf seems to be considerable more effective than Y in limiting scale cracking on the NiCrAl alloys. A similar trend is also evident on the CoCrAl alloys.

Thousand-hour cyclic oxidation tests were performed on the same four alloys for comparison with the AE data. Each cycle consisted of 45 minutes

isothermal oxidation followed by 15 minutes cooling outside the furnace. The weight change versus time data for the four alloys are presented in Figure 16. Again there is little difference between the two Co-base alloys and both continue to gain weight throughout the test. The Ni-base alloys also gain weight initially but after relatively short times begin to lose weight. The NiCrAlY alloy shows poorer cyclic oxidation behavior than NiCrAlHf which is consistent with the greater scale damage indicated by AE for this alloy on cooling after 24 hours oxidation.

Finally both the acoustic emission data and the cyclic oxidation weight change data show that cracking and spalling of alumina from NiCrAl is more severe than from CoCrAl substrates.

To compare the adhesion of alumina on NiCrAl and CoCrAl substrates more closely acoustic emission tests were performed upon cooling CoCrAl(A) and NiCrAl(C) after oxidation 24 hours at 1050°C. The results are presented in Figure 17 where it can be seen that cracking is detected on the NiCrAl alloy at a higher temperature than the CoCrAl. These results are consistent with the data presented in Figures 15 and 16 which showed that the alumina on CoCrAl-base alloys was more resistant to cracking and spalling compared to NiCrAl-base alloys. It is worth noting that these results are consistent with other data in the literature. For example the data of Giggins and Pettit[3] show that alumina spalls more severely from NiCrAl-base alloys compared to CoCrAl- base alloys.

The reason for the observed difference in the adhesion of alumina on NiCrAl- and CoCrAl- base alloys is not available as yet. It is not related to any oxygen active element effect since it has been observed on these alloys when oxygen active elements were not present. This difference in adhesion must result from greater stresses developed in the scales on NiCrAl

or better bonding of the scale on CoCrAl. The acoustic emission data can also be plotted to attempt to identify different events in the cracking and spalling process. In Figure 18 data are presented where events are plotted as a function of peak amplitude. It can be seen that both alloys exhibit a peak that can be ascribed to cracking, but the NiCrAl alloy appears to have a second peak which may be due to spalling. These results indicate that spalling is much more of a part of the alumina degradation process on NiCrAl than CoCrAl. Cracking of the scale is an event where a crack is formed in the alumina scale normal to the plane of the alumina- alloy interface. Spalling is an event where cracking occurs in the plane of the alumina - alloy interface. Hence the data suggesting that more spalling events take place on NiCrAl than CoCrAl indicate the bonding of alumina to CoCrAl may be better than to NiCrAl-base alloys.

The results presented in Figures 15 and 16 indicate that Hf is more effective in promoting the adherence of alumina to alloys than yttrium. To compare the effects produced by these elements in more detail, NiCrAl - and CoCrAl- base alloys with 0.3% yttrium were prepared and tested in cyclic oxidation and acoustic emission measurements were also performed. The results are compared to alloys with hafnium in Figure 19. As in the case of results presented previously the acoustic emission data show that more damage occurs in the alumina formed on NiCrAl- based alloys compared to CoCrAl - base alloys. However in contrast to the data presented in 15 and 16, the results show more damage in alumina formed on NiCrAlHf compared to NiCrAlY. The acoustic emission results are supported by results obtained from cyclic oxidation, Figure 20. There seems to be a similar trend with the CoCrAl - base alloys but the damage is so small that a significant difference cannot be discussed with confidence. The nominal yttrium content of the

NiCrAlY and CoCrAlY alloys for which the data of Figure 19 were obtained was 0.3% whereas it was 0.2% for the data presented in Figure 15 and 16. These results show that the yttrium concentration is a significant parameter in determining the amount of damage that is developed in alumina scales on NiCrAlY and CoCrAlY during cyclic oxidation.

It is worth noting that in the case of the NiCrAl alloys the acoustic emission counts presented in Figure 19 become greater as the number of cycles (i.e. the number of times specimens were cooled to room temperature) was increased. A similar trend is not evident in the CoCrAl alloys probably because the amount of damage in the alumina scales is much less. These results indicate that acoustic emission may be used to compare the amount of damage that is developed or accumulated in alumina scales on alloys. This technique possibly can be used as a nondestructive test to determine the amount of useful life which remains in alumina-forming coatings on alloys.

While the present program is concerned with the adherence of alumina on alloys, many alloys develop resistance to oxidation by using Cr_2O_3 scales. Previous studies on Cr_2O_3-forming alloys have shown that Ce additions to the alloy[4] or application of CeO_2 powder to the alloy surface prior to oxidation[5] markedly decrease the rate of oxidation and improve the scale adherence. The acoustic emission technique was used to study the behavior of alloys K (Ni-50Cr) and L(Ni-50Cr-0.1Ce) and a specimen of alloy which had been coated with CeO_2 powder by dipping the specimen in a slurry of CeO_2 in methanol. The alloys were oxidized for 24 hours in air at 1000°C and cooled in the furnace. The AE data obtained during cooling of these alloys are presented in Figure 21. The AE counts recorded for Ni-50Cr are approximately two orders of magnitude greater than those recorded for the Ce-containing or CeO_2-coated alloys. These data are consistent with SEM observations of the specimen surfaces

(Figure 22). The Ni-50Cr alloy Figure 22a) contains large areas from which the scale has spalled revealing smooth areas where the alloy and oxide were separated during oxidation and numerous voids along alloy grain boundaries. The other two alloys exhibit relatively uniform, fine-grained Cr_2O_3 scales. These data indicate that the Ce and CeO_2 produce a marked decrease in the scale damage when Cr_2O_3-forming alloys are cooled. However, the results are not straightforward since the scales on the Ni-Cr-Ce and Ni-Cr-CeO_2 alloys are much thinner than those on the Ce-free alloy because both Ce additions and CeO_2application greatly reduce the growth rate of Cr_2O_3[4, 5]. Therefore, additional experiments in which different oxidation times are used to produce the same scale thicknesses are required to ascertain if the scales on the Ce-modified alloys are indeed more adherent.

In Figure 23 cyclic oxidation results are presented for the above Ni-Cr alloys at 1100°C. The Ni-50Cr alloy is observed to lose weight rapidly from the first cycle whereas the Ni-50Cr-0.1Ce alloy initially gains weight and then begins to lose weight slowly. Some of this weight loss may be due to CrO_3 evaporation but some is also due to cracking and spalling of the Cr_2O_3 scale. The Ni-50Cr+CeO_2 alloy also loses weight but at a slower rate than the Ni-50Cr alloy. These results show that alloy with Ce maintains a protective scale for a longer time than both the Ni-50Cr and Ni-50Cr + CeO_2 alloys.

The acoustic emission results obtained with the chromia-forming alloys show that this technique can be used to indicate damage in chromia scales as well as alumina scales. The weight change data presented in Figure 23 show that the alloy containing Ce is better than the alloy with the CeO_2 slurry. The same results cannot be drawn from the acoustic emission data in Figure 21, however these data do show that the chromia which formed on the alloy with the CeO_2 slurry does begin to crack at a higher temperature than the alloy

with the Ce addition. The acoustic emission data have been obtained for 24 hrs. of oxidation. Additional cycles may permit the acoustic emission technique to be used to differeniate between the damage in the chromia formed on these two specimens.

Experiments were also performed in which it was attempted to measure acoustic emission counts during the isothermal growth of alumina and chromia scales. Significant, reproducible data could not be obtained, however, in the case of columbium oxide scales meaningful data were obtained[6].

In addition to the acoustic emission measurements and the cyclic oxidation testing, tests were also performed in which it was attempted to measure the load required to pull the alumina scales from their substrates.

In this test an epoxy coated stud (1/16 in. dia.) was attached to the oxidized surface of the specimen. The epoxy bond was strengthened by curing in an oven for about one hour at 150°C. After bonding the load required to pull the oxide scale with stud from the specimen was measured by using the fixture shown in Figure 24.

It was hoped that the loads required to pull oxide scales from substrates could be compared and a relation between scale adhesion and the thermal cycling resistance of the alloy could be developed. In addition this test would permit the surfaces of the alloy and the oxide scale at the alloy-alumina interface to be studied with optical and scanning electron microscopy. A problem with this test was that for loads in excess of 10,000 psi failure occurred in the epoxy. In addition, this test could not be used on cyclicly oxidized specimens because the epoxy would flow into cracks in the oxide scale that formed during cyclic oxidation and it was not possible to pull the remaining fragments of oxide scale from the surfaces of specimens.

Some typical results obtained from pulling alumina scales from alloys

are presented in Table III. It can be seen that the loads required to pull the scales from the NiCrAl-0.2Y alloy were less than those for the NiCrAl-0.3Y alloy. These results are in agreement with the acoustic emission that showed more adherent scales were formed on NiCrAl-0.3Y specimens. Other trends which appear to be evident are that the load to pull the scale from the substrate decreases as

-the oxidation time is increased

-the specimen cooling rate is decreased

-the specimen surface finish becomes more rough.

These results show that the load to pull scales from alloy surfaces can be used to compare the effects of alloy composition, specimen surface condition and oxide scale thickness on the oxide scale adherence. It is expected that this procedure can be used to also study the effects of other parameters which influence oxide scale adhesion. It is important to note that in all cases where the acoustic emission test and the oxide stripping test where used on the same specimens, consistent results were obtained. The results obtained with the NiCrAl-0.2Y(D) and NiCrAl-0.3Y(E) specimens show that the oxide scale adherence is dependent upon yttrium concentration. In Figure 25 the surfaces of such alloys can be seen after the alumina scales which formed during oxidation were removed. Much fewer oxide pegs are evident in the alloy with 0.3Y. This condition is confusing since the number of pegs should increase with yttrium concentration. These alloys and the stripped scales (Figure 26) are being studied to determine why the alloy with 0.3Y has better scale adherence than the alloy with 0.2Y.

SIGNIFICANT RESULTS OBTAINED IN THIS PROGRAM

The results which have been obtained during the past year which are considered to be significant are discussed briefly in the following:

1. Silica scales have been formed on nickel-silicon alloys which have growth rates substantially less than those for alumina scales formed under similar conditions. These scales, based upon growth rate considerations, are believed to represent a significant potential for use as barriers on coatings on high temperature alloys in place of alumina scales which are formed on present state-of-the-art MCrAlY coatings.
2. Techniques have found which can be used to characterize oxide scale adhesion more precisely than cyclic oxidation tests. These techniques are:
   - ·acoustic emission
   - ·measuring loads to strip oxide scales from substrate surfaces
3. These techniques can now be used to define the parameters (i.e. oxygen active element concentration, type of oxygen active element, surface condition, etc.) which must be controlled in order to optimize alumina scale adhesion on alloys, and to develop a non-destructive test to determine the useful lives of coatings on alloys which remain after use under service conditions.
4. Using these techniques it has been demonstrated that the following parameters affect alumina scale adherence:
   - -oxygen active element type and concentration
   - -base alloy composition (e.g. nickel-versus cobalt-base)

-alloy surfaces condition

-specimen cooling rate

-exposure time of specimen to oxidation conditions.

5. The mechanism(s) by which the oxygen active elements improve oxide scale adhesion is (are) not totally clear. The data which are being accumulated by studying alumina adherence via the utilization of a variety of techniques should help to clarify this controversial situation.

WORK TO BE PERFORMED DURING THE FOURTH YEAR OF THE PROGRAM

During the fourth year of this program the following work is planned:

1. Conclusive definition of the silica scales formed on nickel-silicon alloys whose growth rates are significantly less than those of alumina formed under similar conditions.
2. Thorough characterization of the acoustic emission technique as a means of nondestructively describing the useful life which remains in an alumina-forming coating on an alloy.
3. Definition of yttrium concentration and distribution in alloys which gives optimum alumina adherence.
4. Comparison of effectiveness of yttrium versus hafnium to improve oxide scale adherence.
5. Preparation of mechanistic description of the effects which the oxygen-active elements exert on oxide scale adherence.

REFERENCES

1. Y. Oya and T. Suzuki, Zeitschrift fer Metallkunde, 74, 21 (1983).

2. G. H. Meier and F. S. Pettit, "Fundamental Research Directed to Advanced High Temperature Coating Systems Beyond the Current State-of-the-Art Systems," University of Pittsburgh, Second Annual Report on AFOSR Contract No. 1 AFOSR-80-0089, April 1, 1982.

3. C. S. Giggins and F. S. Pettit, ARL-TR-75-0234, PWA-5364, AD-A024104, Pratt and Whitney Aircraft Co., 1975.

4. G. M. Ecer and G. H. Meier, Oxid. Met. 5, 159, 1979.

5. G. M. Ecer, R. B. Singh and G. H. Meier, Oxid. of Metals, 18, 53, 1982.

6. G. H. Meier and R. Perkins, Extended Abstracts of the Spring (1983) Meeting of the Electrochemical Society.

TABLE I

COMPOSITIONS OF NICKEL-SILICON ALLOYS

ALLOY	WEIGHT-PERCENT SILICON
Ni-5Si	5
Ni-7.5Si	7.5
Ni-10Si	10
Ni-12.5Si	12.5
*Ni-15Si	15
Ni-20Si	20

*The Ni-15Si alloy contained porosity which apparently resulted in oxidation rates for this alloy close to those for the Ni-5Si.

TABLE II

NOMINAL COMPOSITIONS OF THE ALLOYS STUDIED (WT.%)

ALLOY DESEGNATION	Ni	Co	Cr	Al	Y	Hf	Ce
A. CoCrAl	-	Bal	22	11	-	-	-
B. CoCrAlY	-	Bal	22	11	0.5	-	-
C. NiCrAl	Bal	-	20	10	-	-	-
D. NiCrAlY	Bal	-	20	10	0.2	-	-
E. NiCrAlY	Bal	-	20	10	0.3	-	-
F. NiCrAlHf	Bal	-	20	10	-	1	-
G. CoCrAl	-	Bal	20	10	-	-	-
H. CoCrAlY	-	Bal	20	10	0.2	-	-
I. CoCrAlY	-	Bal	20	10	0.3	-	-
J. CoCrAlHf	-	Bal	20	10	-	1	-
K. Ni-50Cr	Bal	-	50	-	-	-	-
L. Ni-50Cr-0.1Ce	Bal	-	50	-	-	-	0.1

TABLE III

LOADS REQUIRED TO PULL ALUMINA SCALES FROM ALLOYS (KSi)

	24 hrs.	48 hrs.	100 hrs.*
NiCrAl-0.3Y			
600 grit Polish, Fast Cool**	9.59	9.46	7.66
0.05 μm Polish, Fast cool	9.88	-	9.01
600 grit Polish, Slow cool	-	8.83	-
NiCrAl - 0.2Y			
600 grit Polish, Fast cool	8.10	6.63	7.48
0.05 μ m Polish, Fast cool	8.32	-	8.63
600 grit Polish, slow cool	-	5.74	-

*Time of isothermal oxidation at 1050°C.

**Cooling rates were as follows: Slow cool was furnace cool.
Fast cool was air cool.

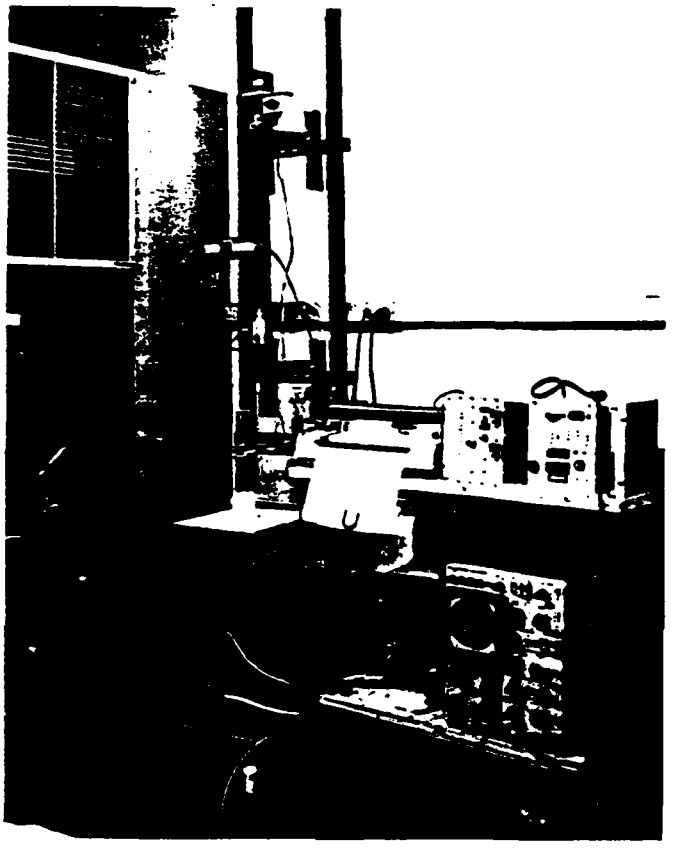

Figure 1. Photograph of acoustic emission apparatus used for studying high-temperature oxidation.

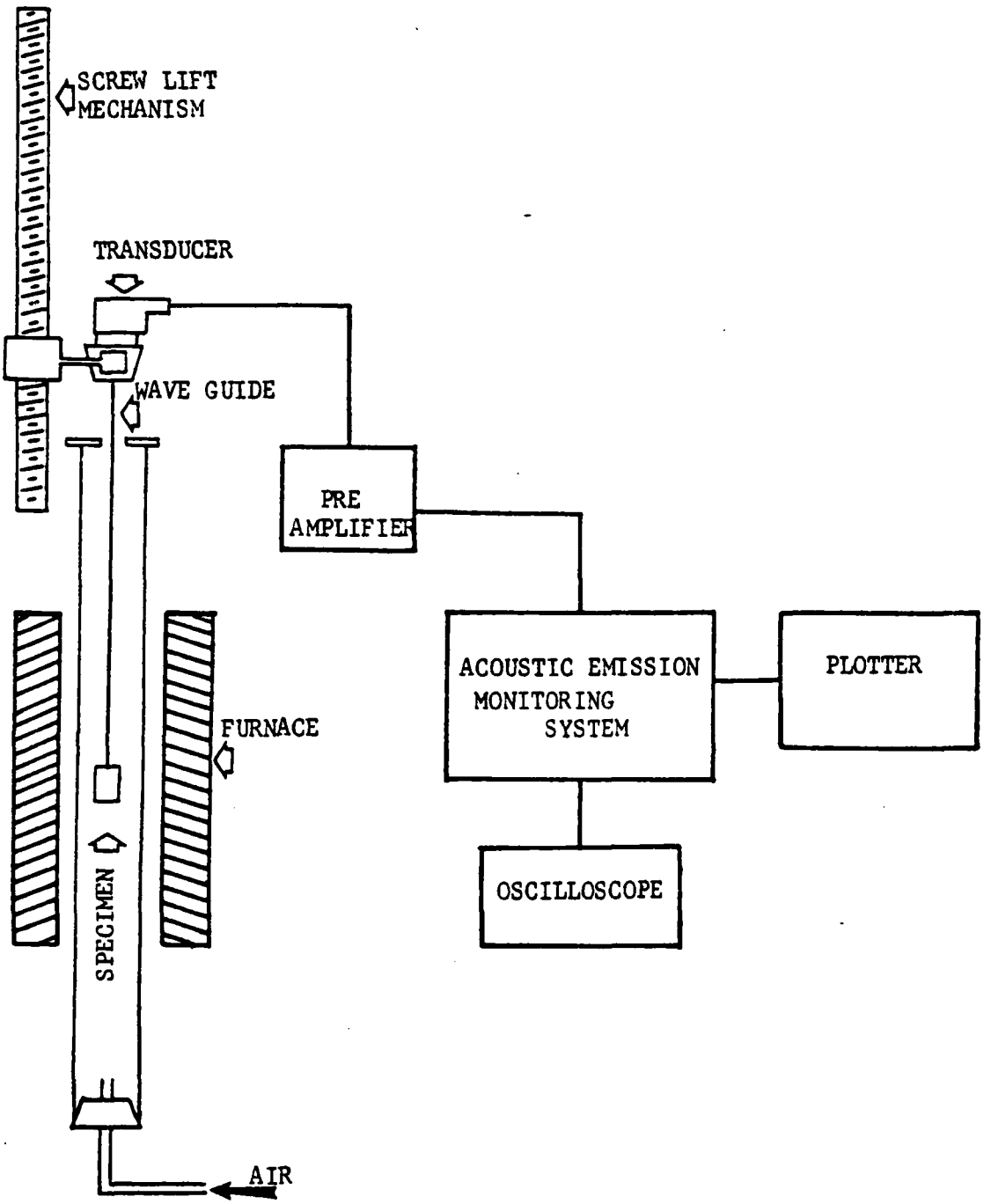

Figure 2. Schematic Diagram of acoustic emission apparatus used for studying high-temperature oxidation.

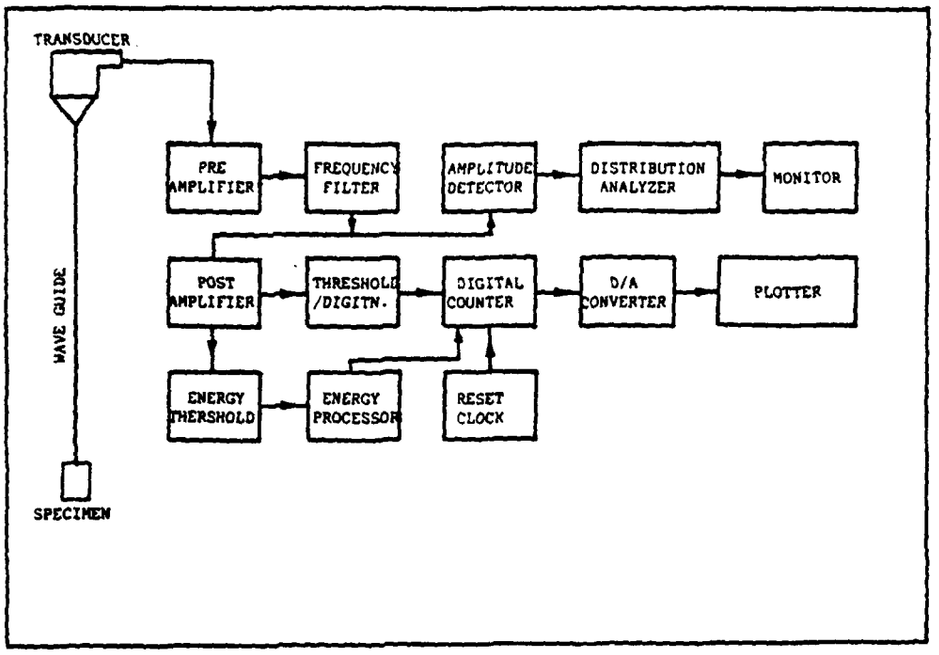

Figure 3. Function block diagram of acoustic emission detection system.

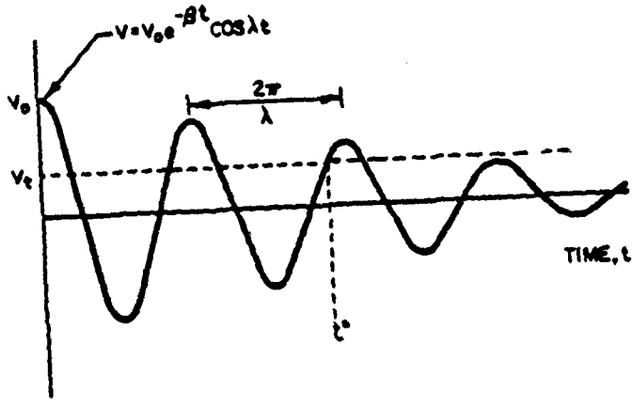

Figure 4. Schematic diagram of "ringing down" of an acoustic emission signal.

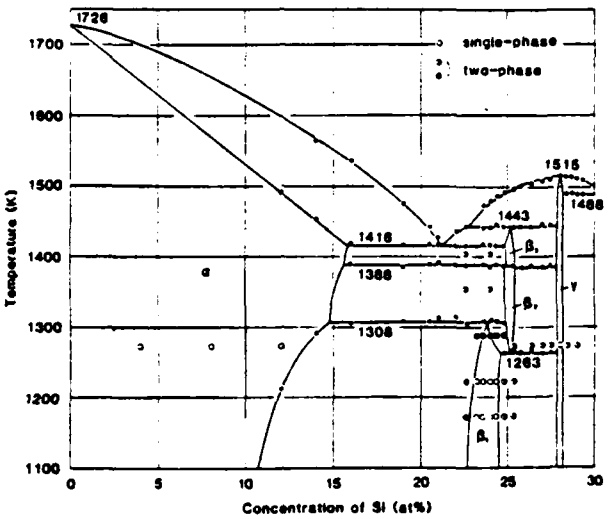

Figure 5. Ni-rich portion of the Ni-Si phase diagram (ref. 1).

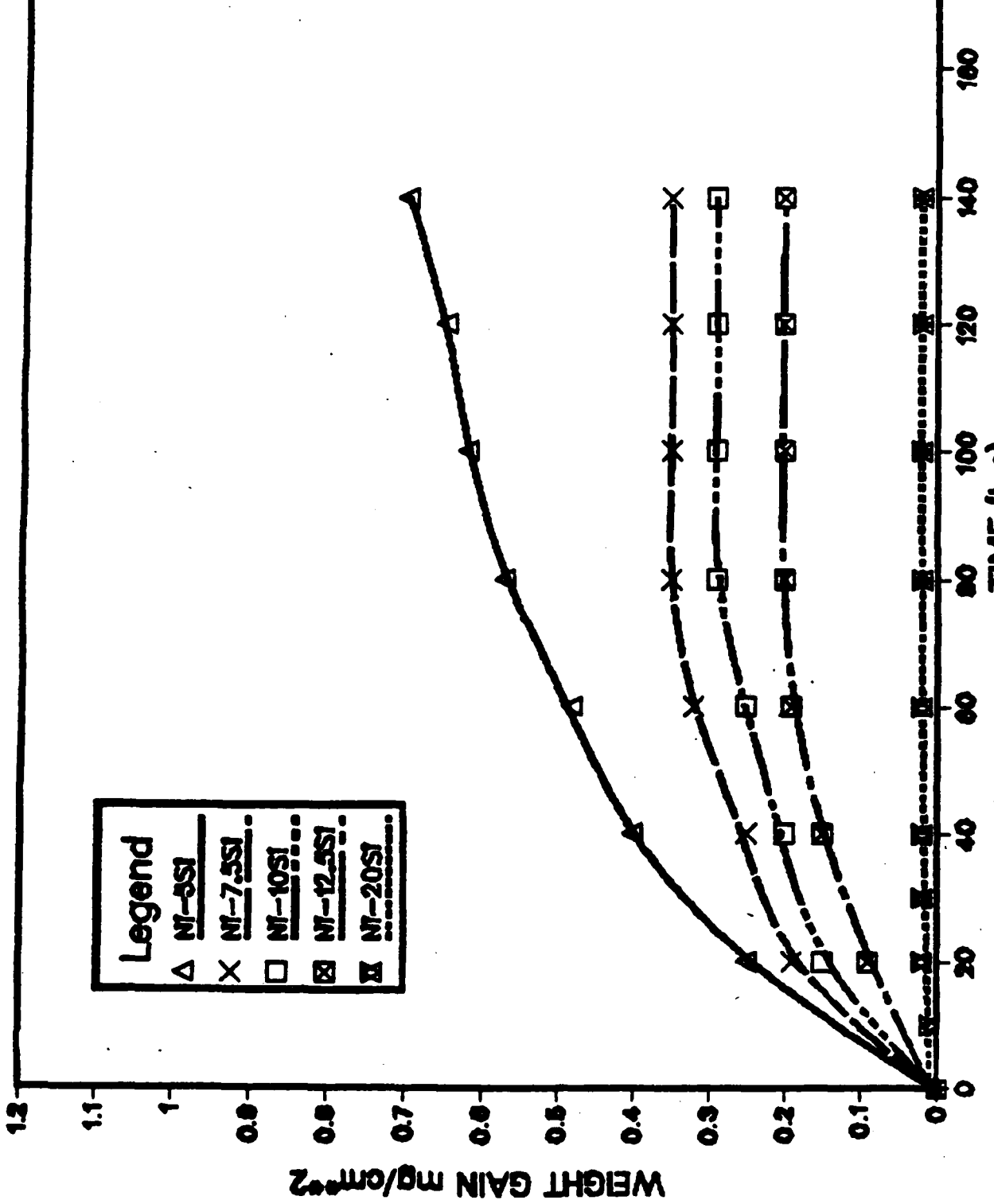

Figure 6. Weight change versus time data for nickel silicon alloys oxidized in air at 900°C.

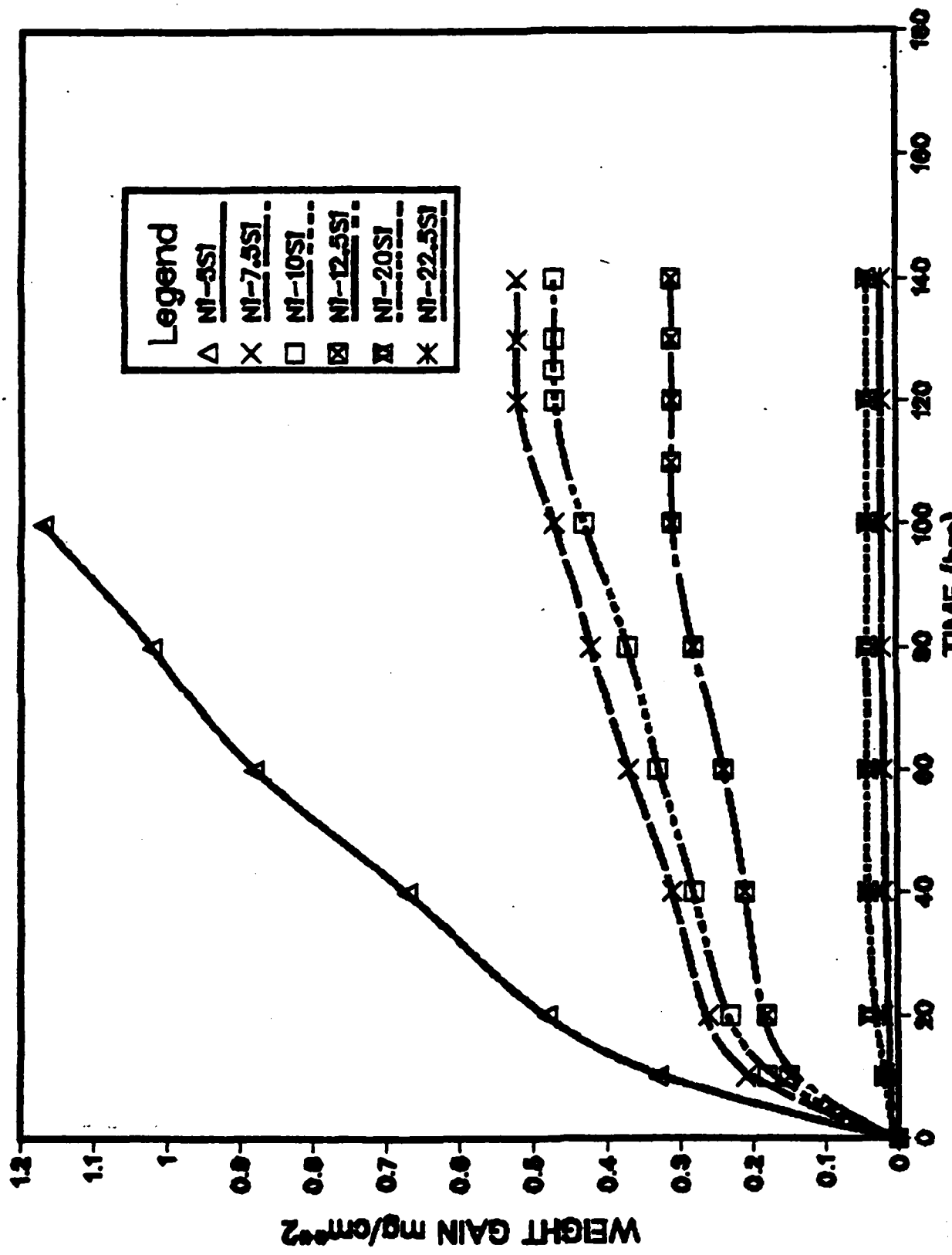

Figure 7. Weight change versus time data for nickel-silicon alloys oxidized in air at 1000°C.

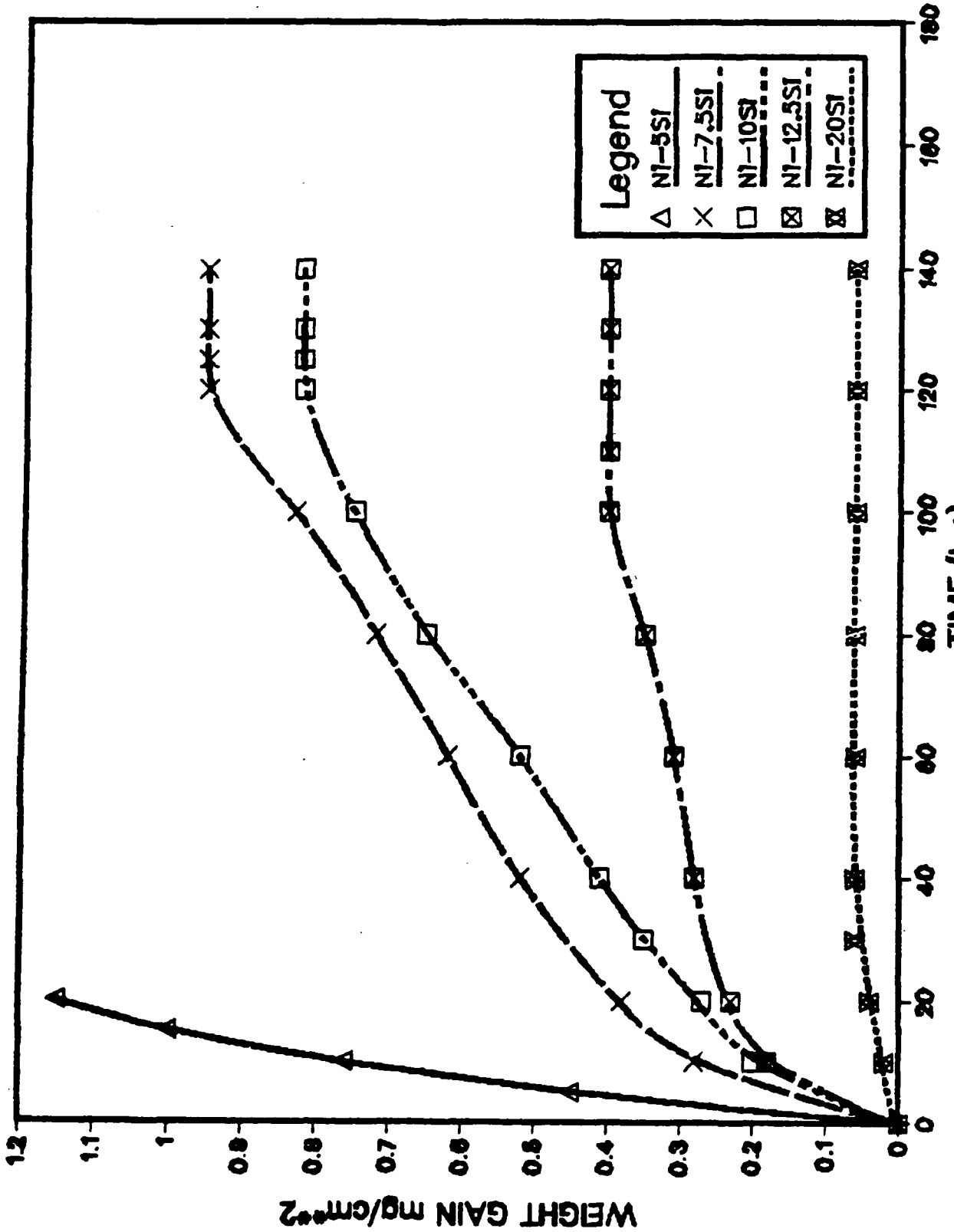

Figure 8. Weight change versus time data for nickel silicon alloys oxidized in air at 1100°C.

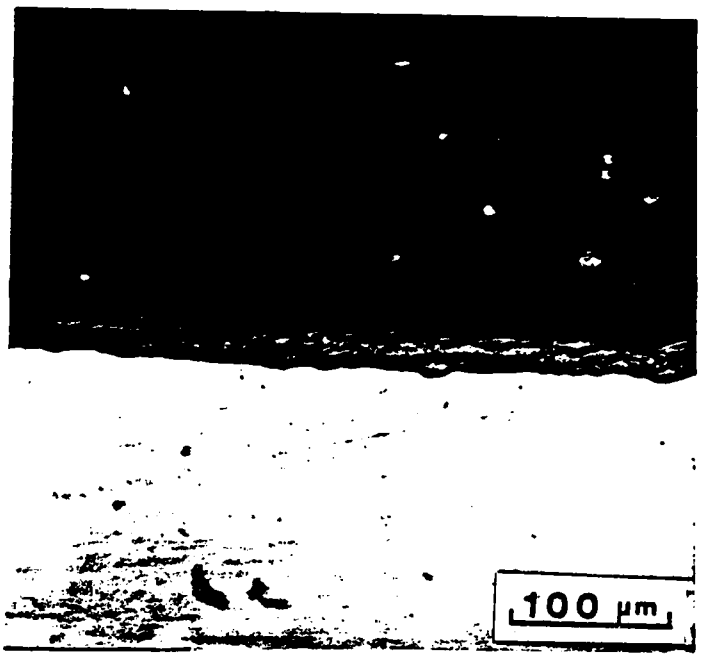

Figure 9. Oxide scale formed upon a Ni-5Si alloy after 168 hours of oxidation at 1100°C in air. The external scale is relatively thick and contains nickel but no internal oxidation of the silicon is evident.

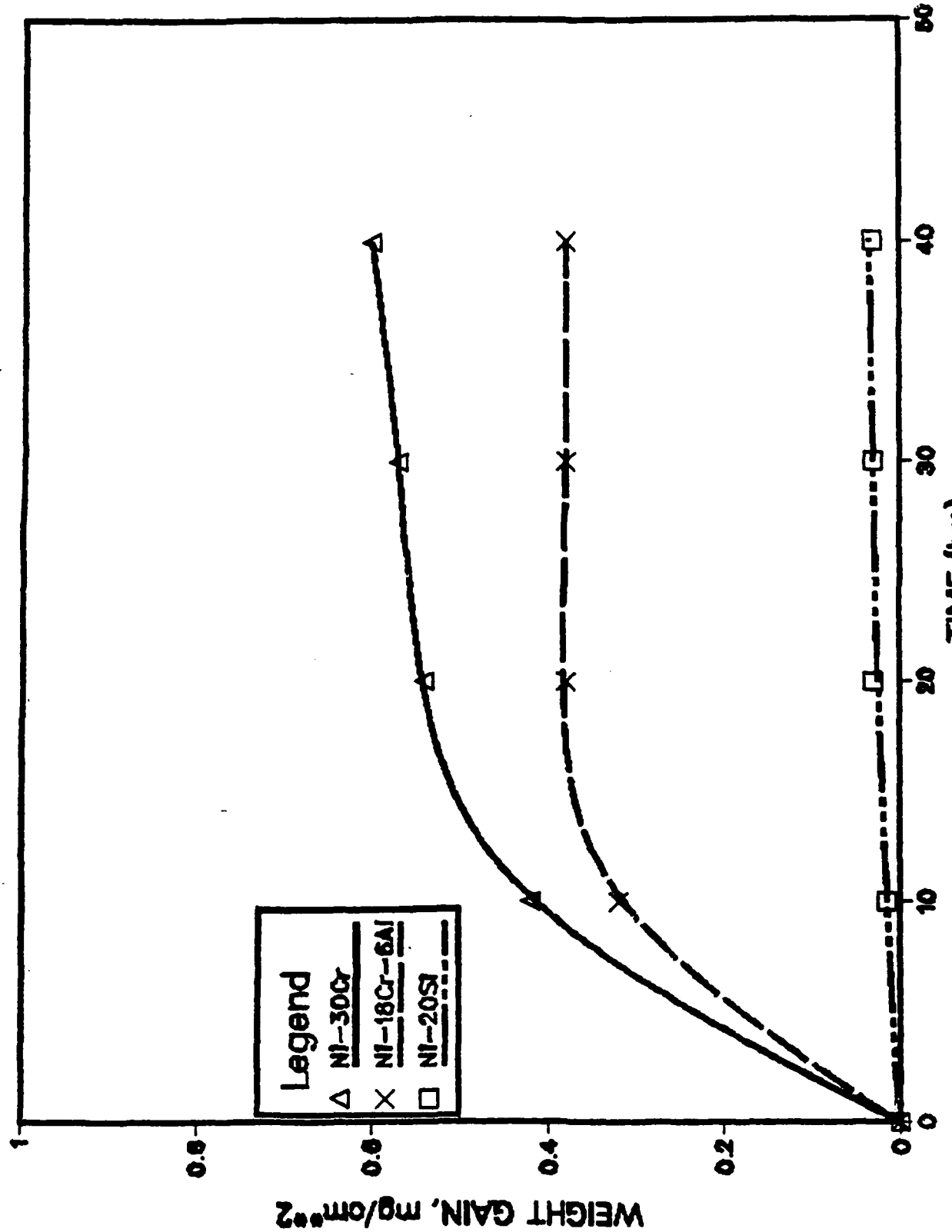

Figure 10. Comparison of weight change data for alloys which depend upon Cr_2O_3(Ni-30Cr), Al_2O_3(Ni-18Cr-6Al) and silica (Ni-20Si) scales for protection(1000°C).

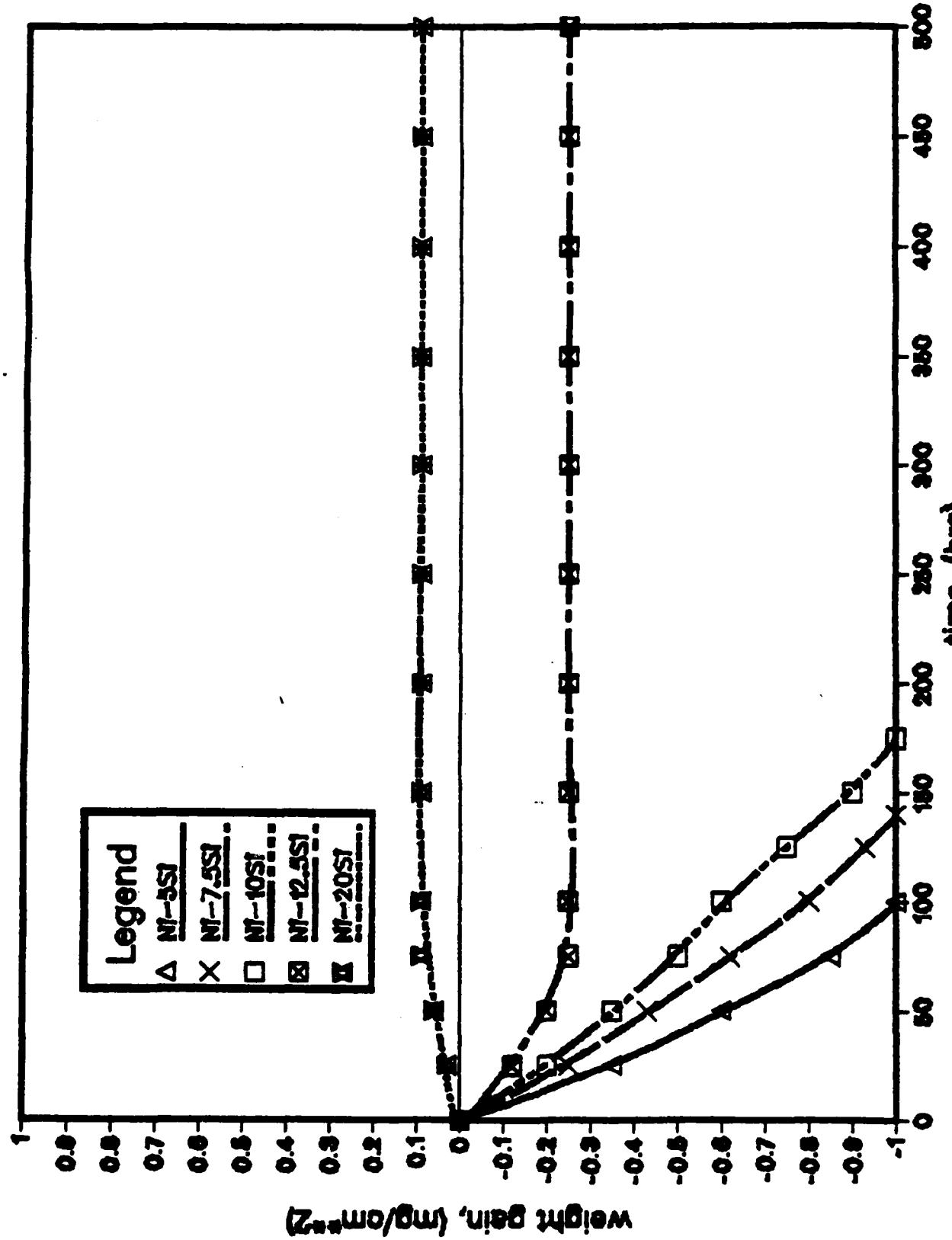

Figure 11. Cyclic oxidation data for Ni-Si alloys at 1000°C in air.

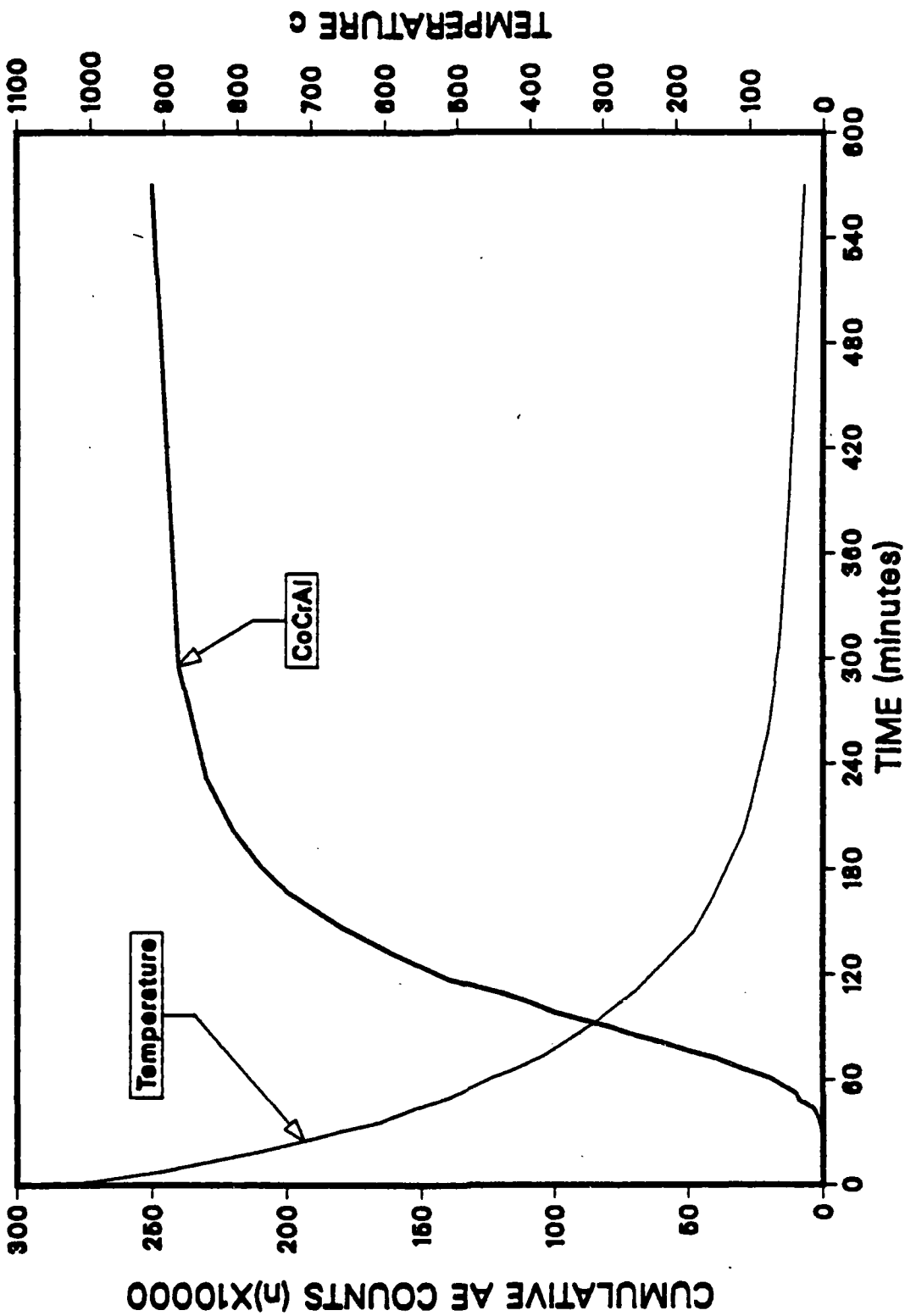

Figure 12. Acoustic emission counts detected during cooling of a Co-22-Cr-11Al alloy after 24 hr oxidation in air at 1050°C.

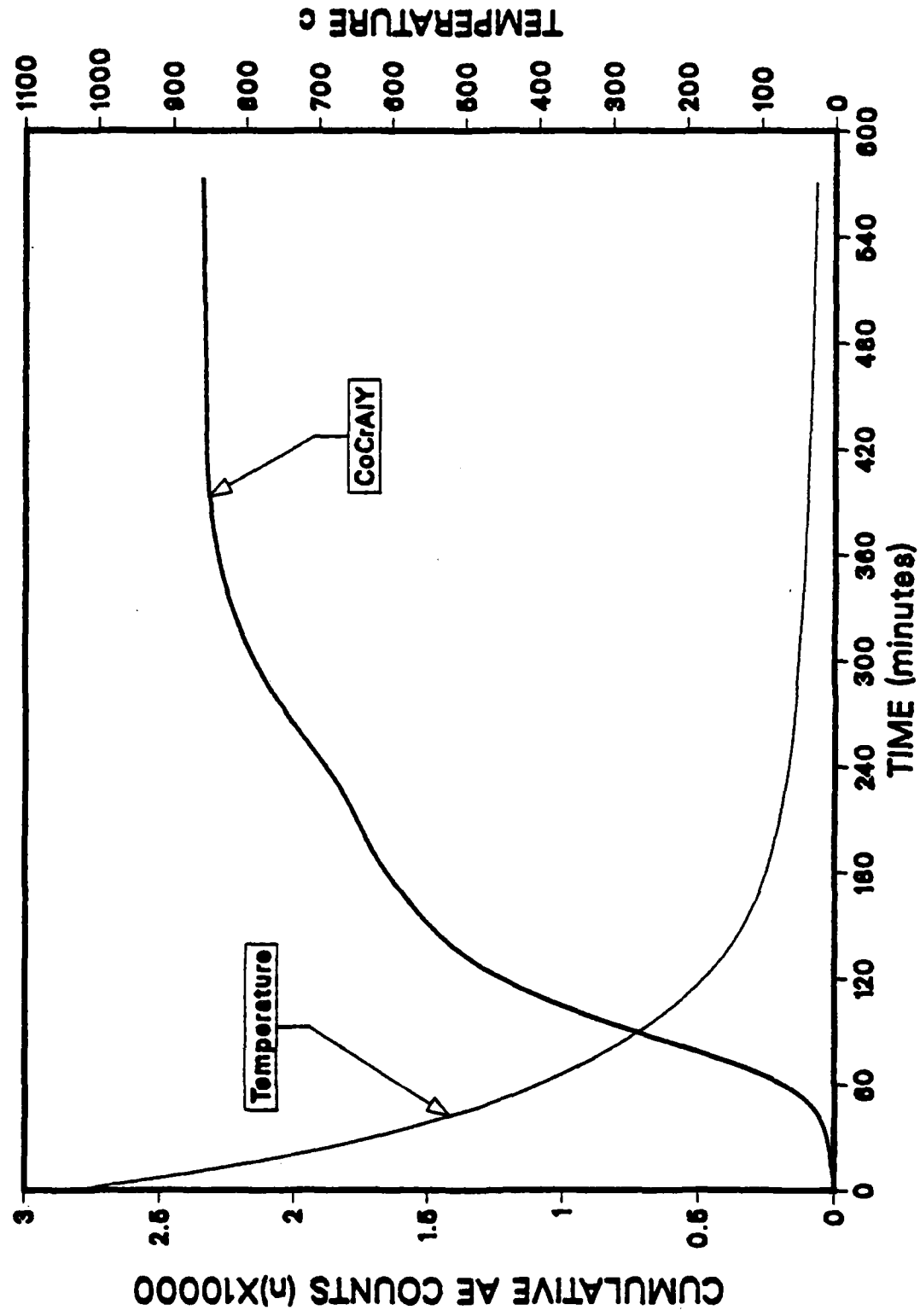

Figure 13. Acoustic emission counts detected during cooling of a Co-22Cr-11Al-0.5Y alloy after 24 hr oxidation in air at 1050°C.

a

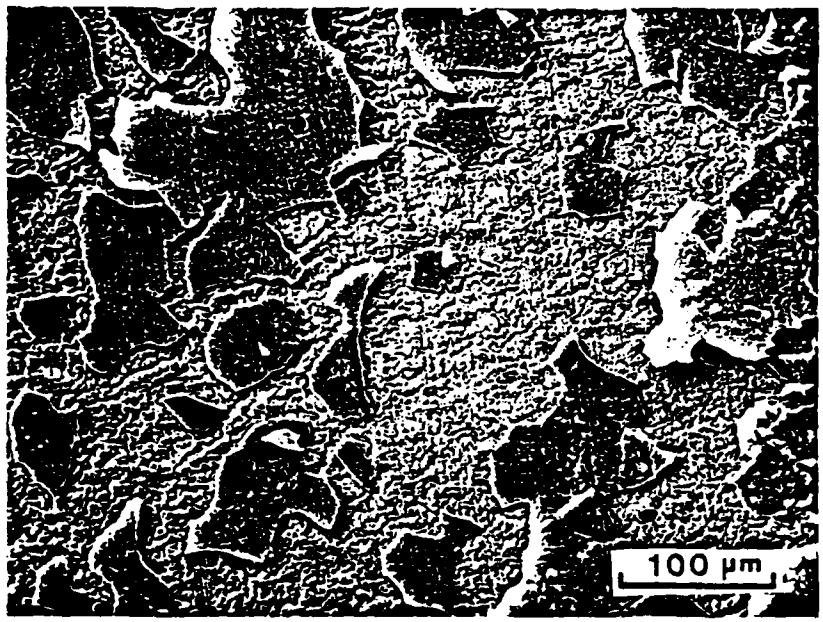

b

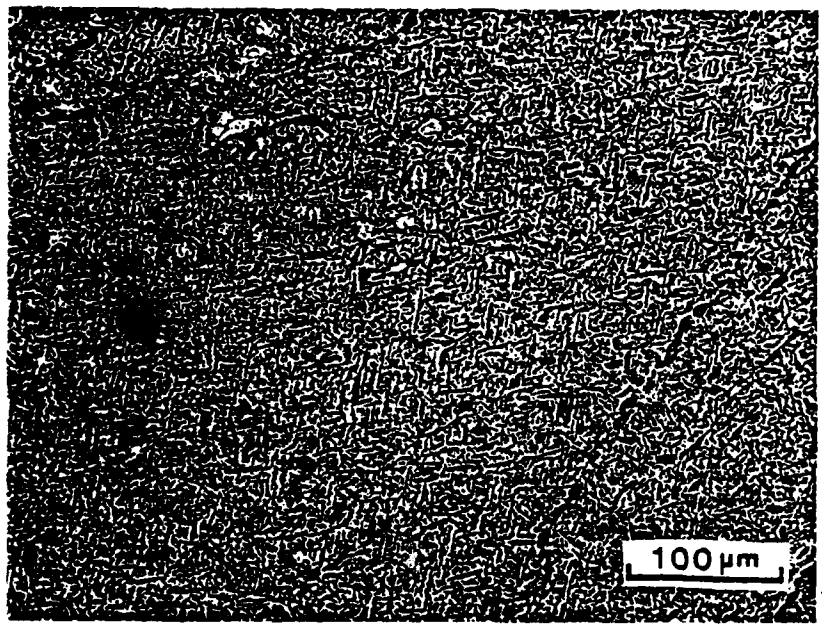

Figure 14. Scanning electron micrographs of the surfaces of specimens oxidized for 24 hrs in air at 1050°C.

a. Co-22Cr-11Al b. Co-22Cr-11Al-0.5Y

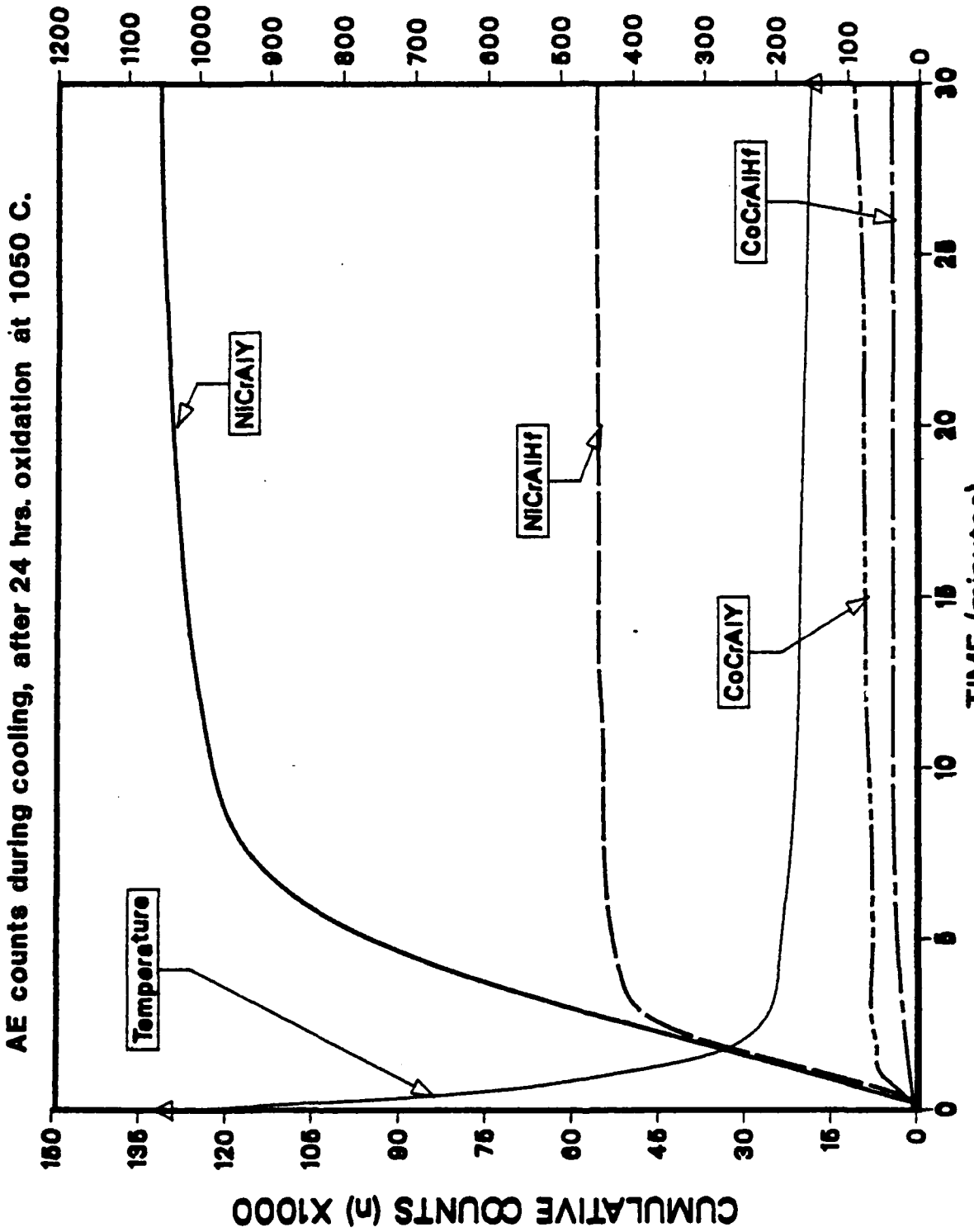

Figure 15. Acoustic emission counts detected during cooling of NiCrAlY, NiCrAlHf, CoCrAlY, and CoCrAlHf alloys after oxidation for 24 hrs in air at 1050°C.

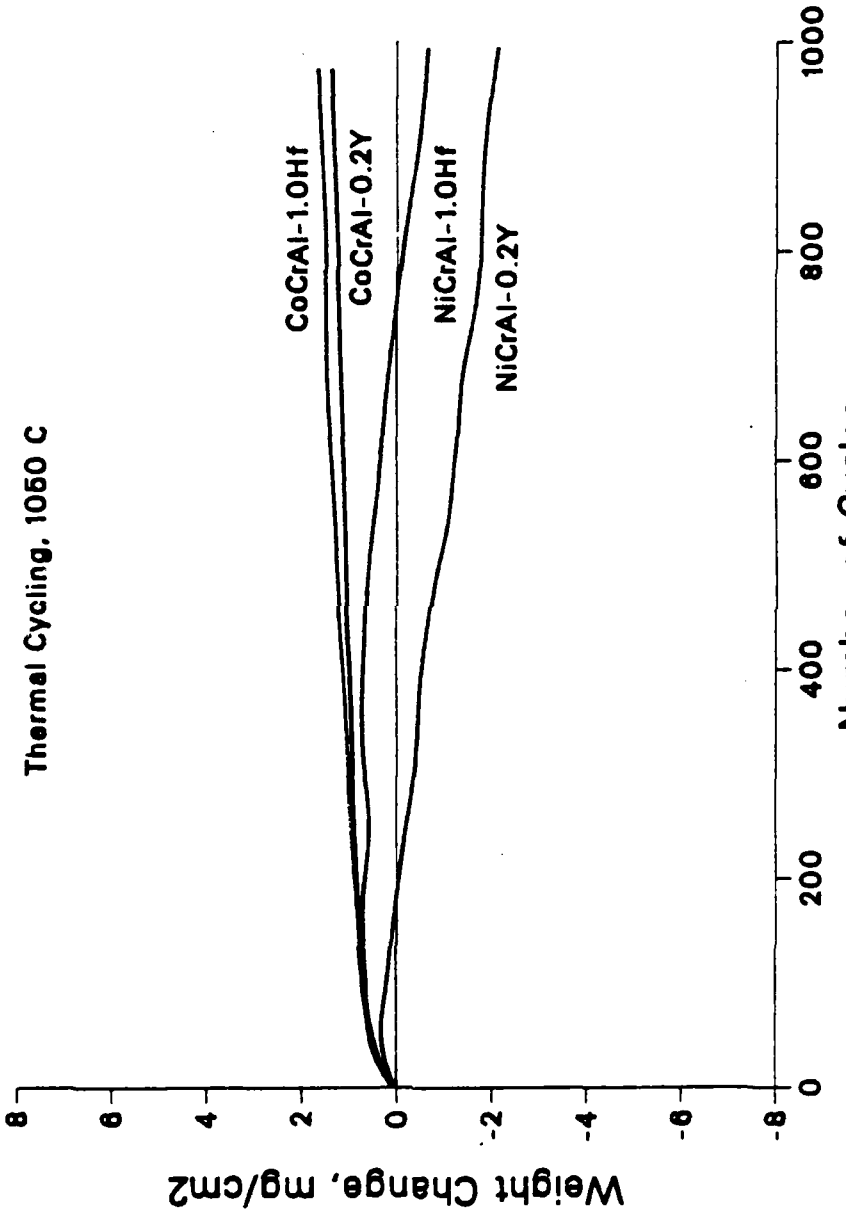

Figure 16. Cyclic oxidation data for some NiCrAl and CoCrAl alloys in air at 1050°C.

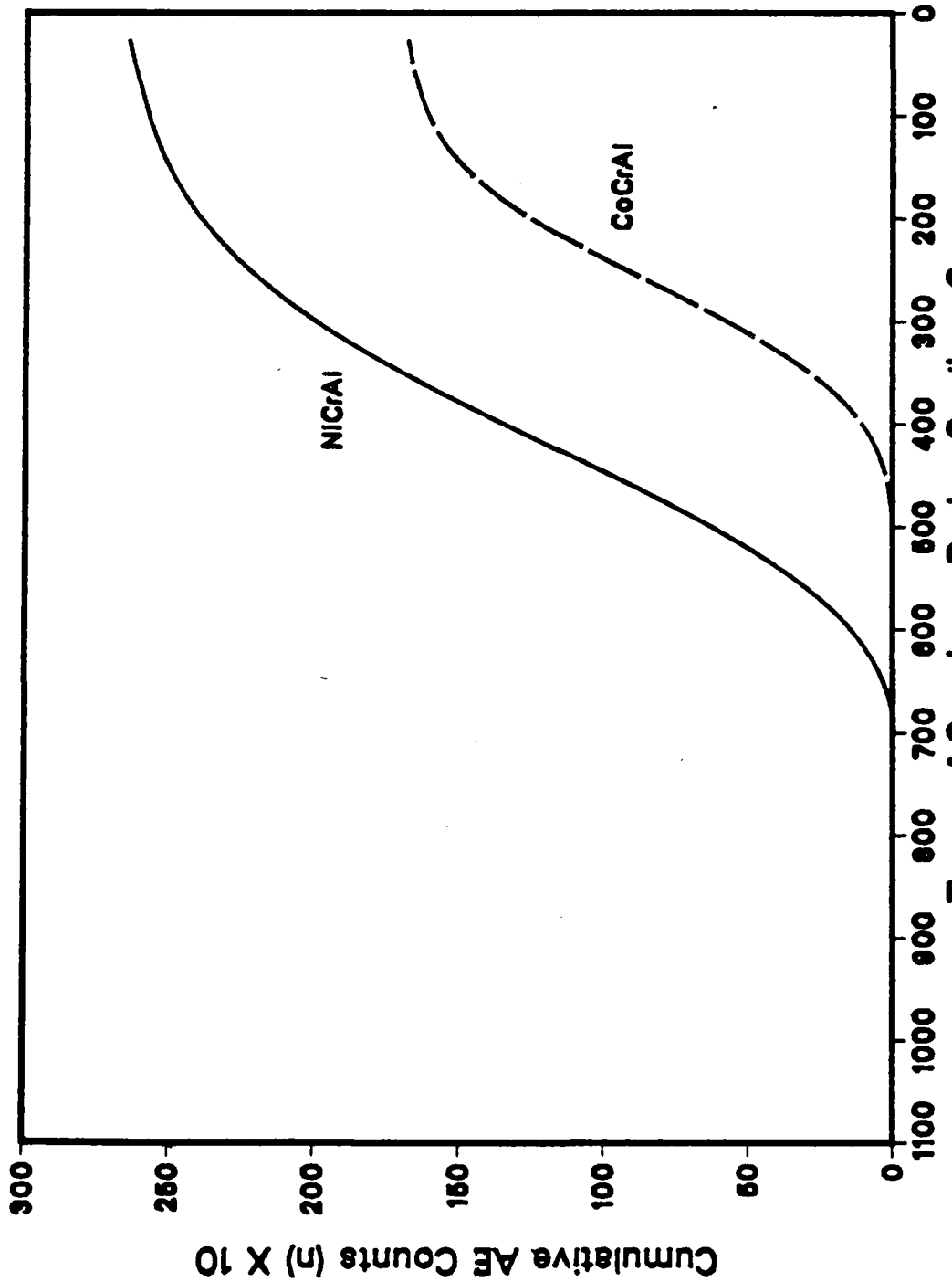

Figure 17. Acoustic emission data obtained upon cooling NiCrAl and CoCrAl specimens after oxidation.

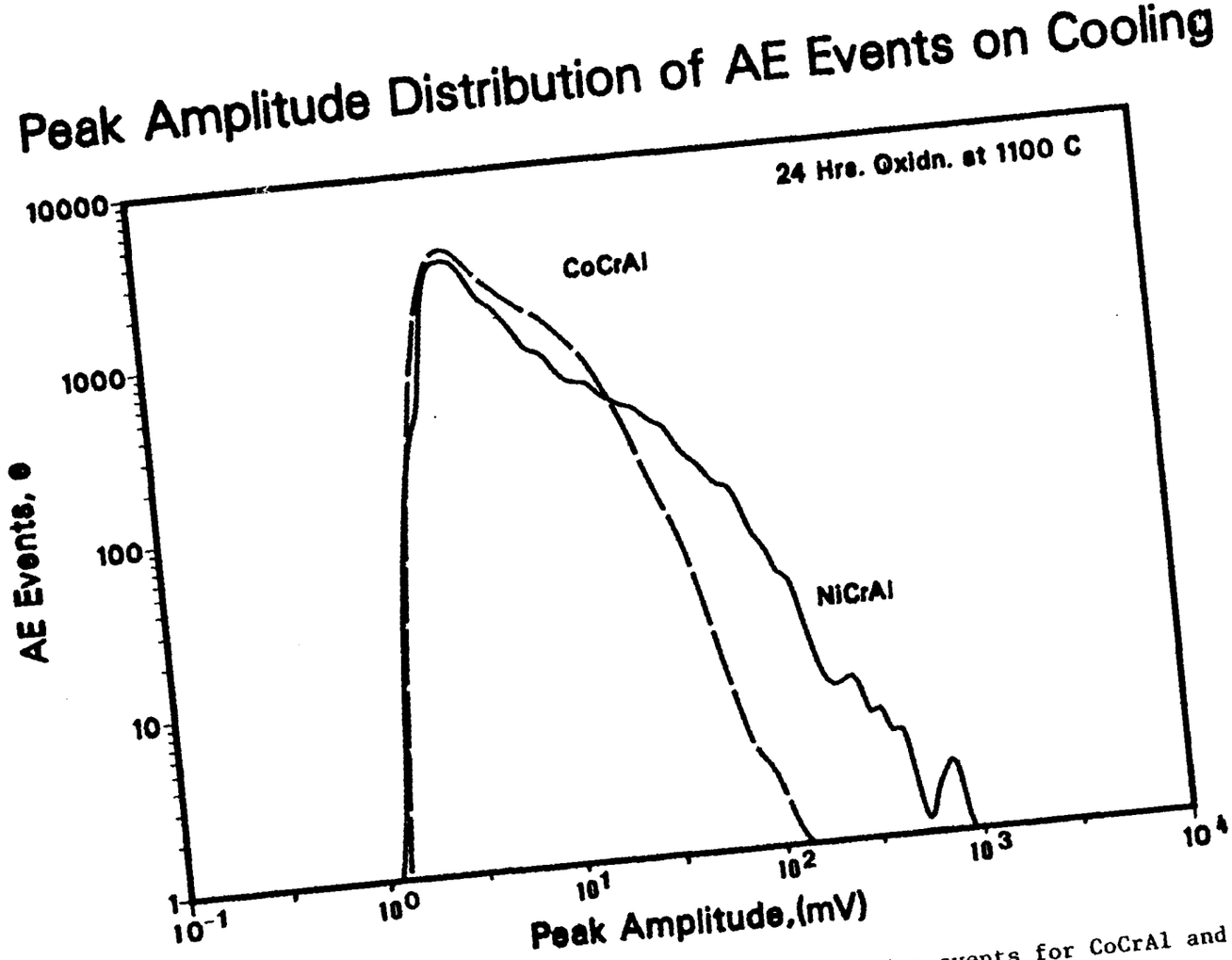

Figure 18. Distribution of the acoustic emission events for CoCrAl and NiCrAl alloys with respect to their peak amplitude, data obtained upon cooling oxidized specimens from oxidation temperature.

Scale Damage during Thermal Cycling

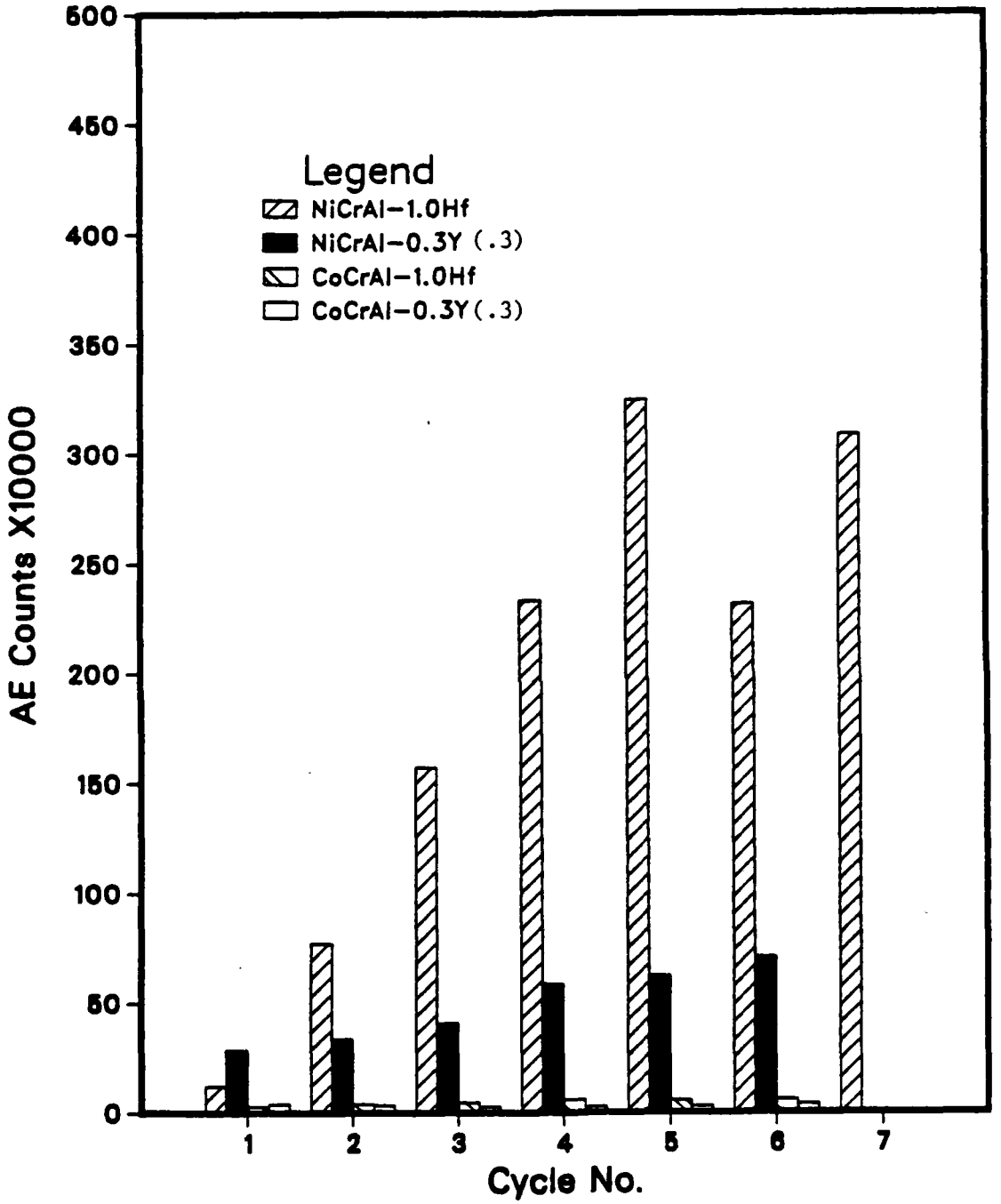

Figure 19. Acoustic emission data obtained for alloys tested in cyclic oxidation (24 hour cycles and oxidation temperature of 1100°C in air. A total gain of 90 dBs used.)

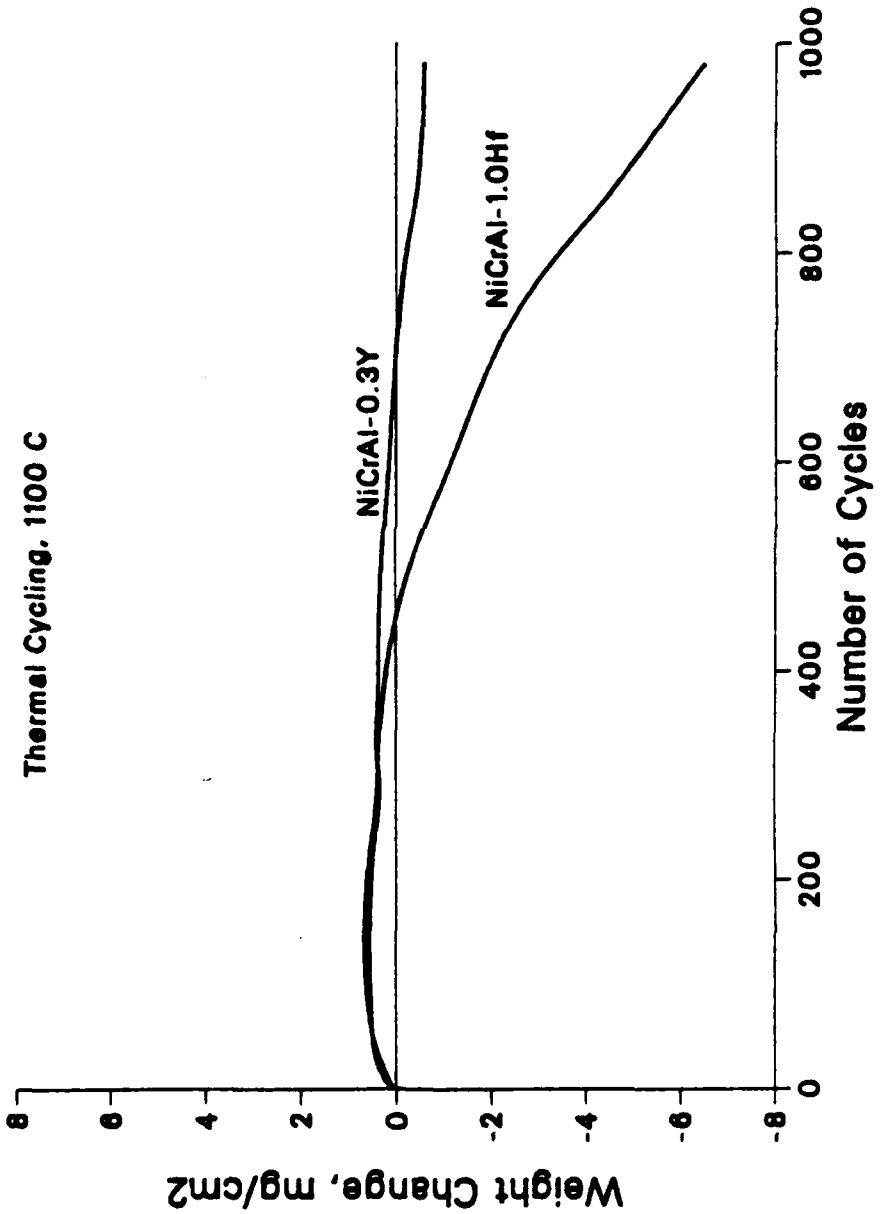

Figure 20. Weight change data for the cyclic oxidation of NiCrAl alloys in air.

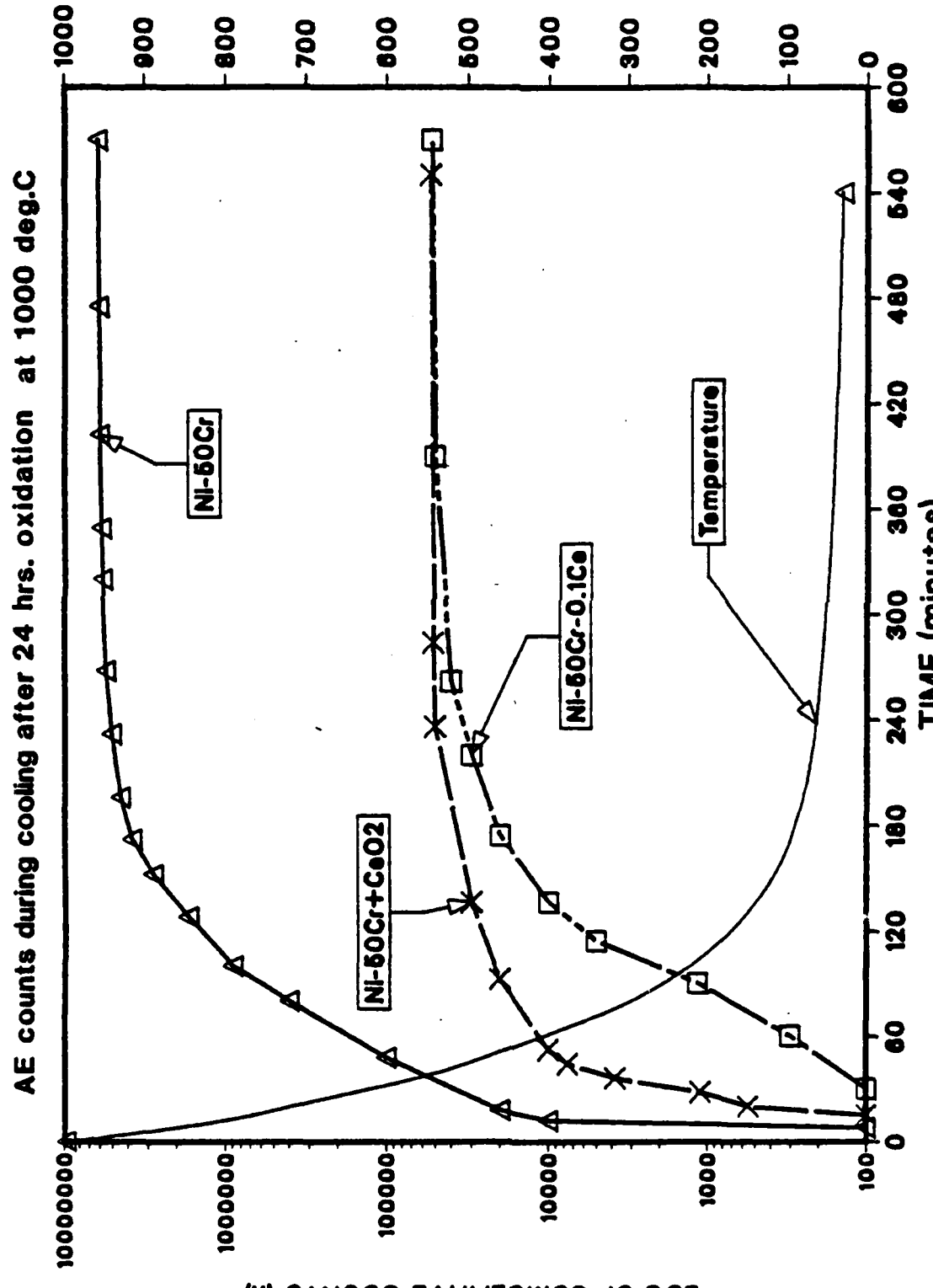

Figure 21. Acoustic emission counts detected during cooling of Ni-50Cr, Ni-50Cr-0.1Ce, and Ni-50Cr + CeO_2 alloys oxidized for 24 hrs in air at 1000°C.

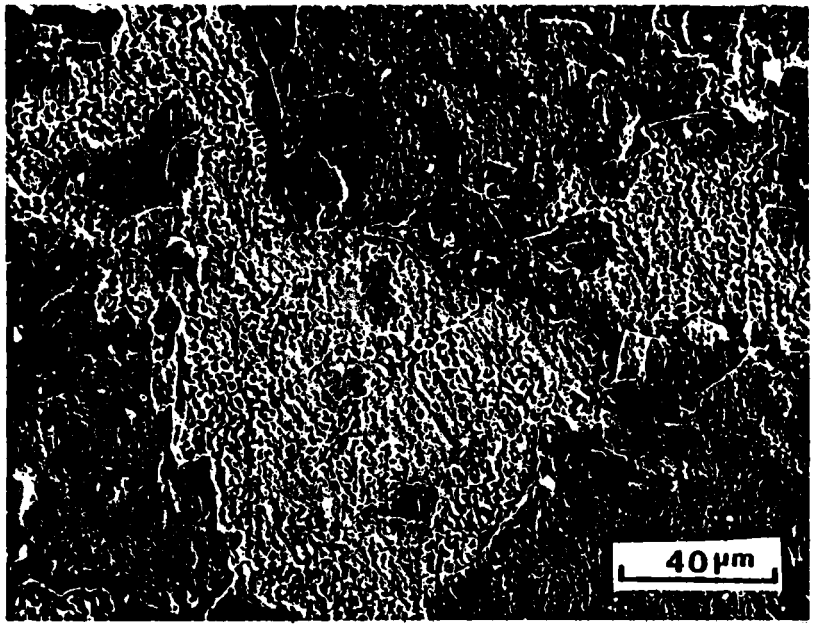

a

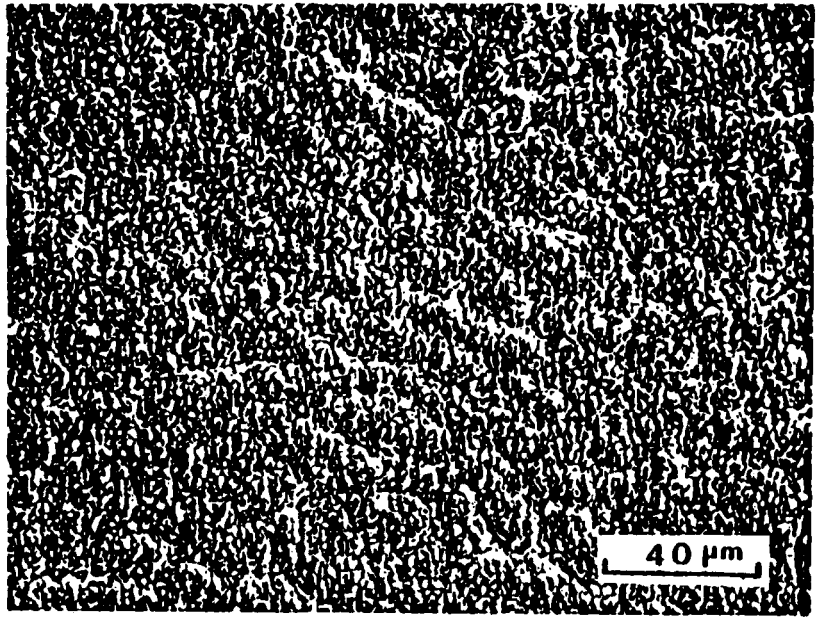

b

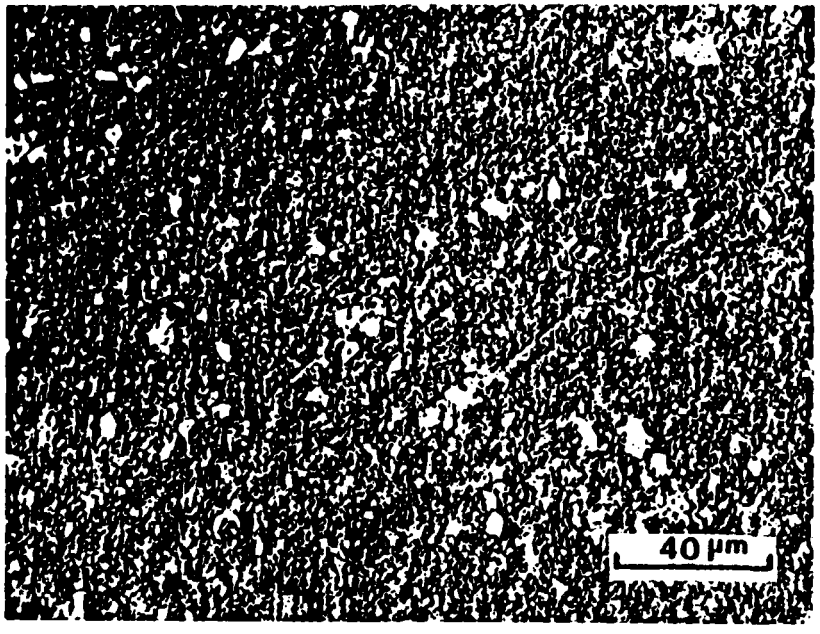

c

Figure 22. Scanning Electron micrographs of alloys oxidized for 24 hrs at 1000°C. A. Ni-50Cr, b. Ni-50Cr-0.5Ce c. Ni-50Cr + CeO_2.

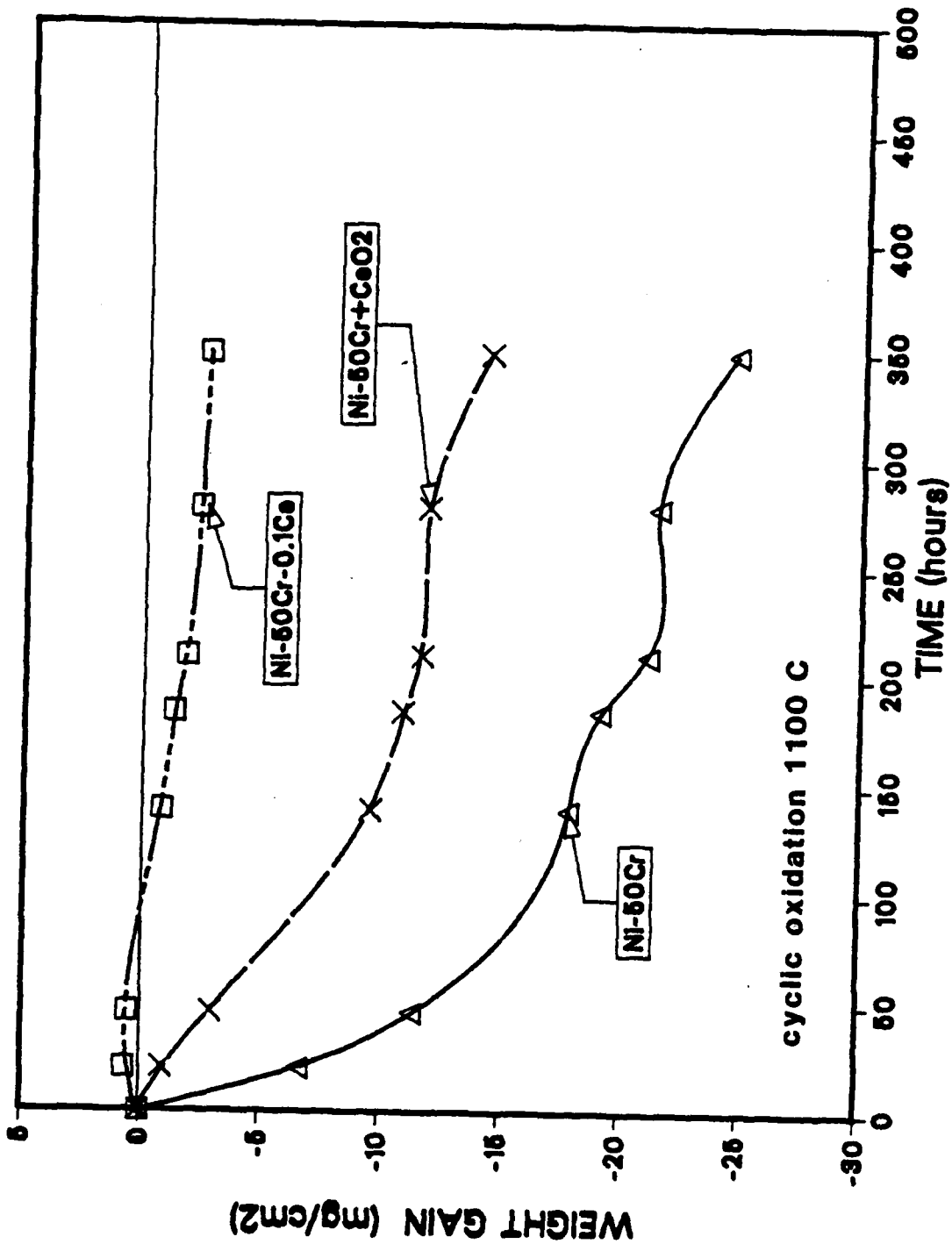

Figure 23. Cyclic oxidation weight changes for several Ni-Cr alloys oxidized in air at 1100°C.

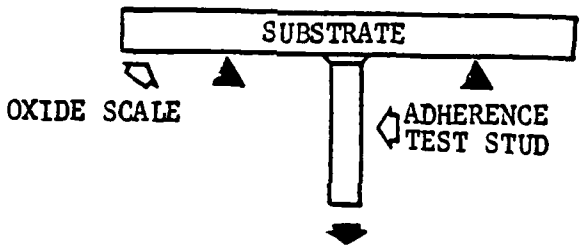

Figure 24. Schematic diagrams showing stud attached to specimen with oxide scale. The arrow beneath the stud indicates the load applied to the stud in order to pull the oxide scale from the substrate.

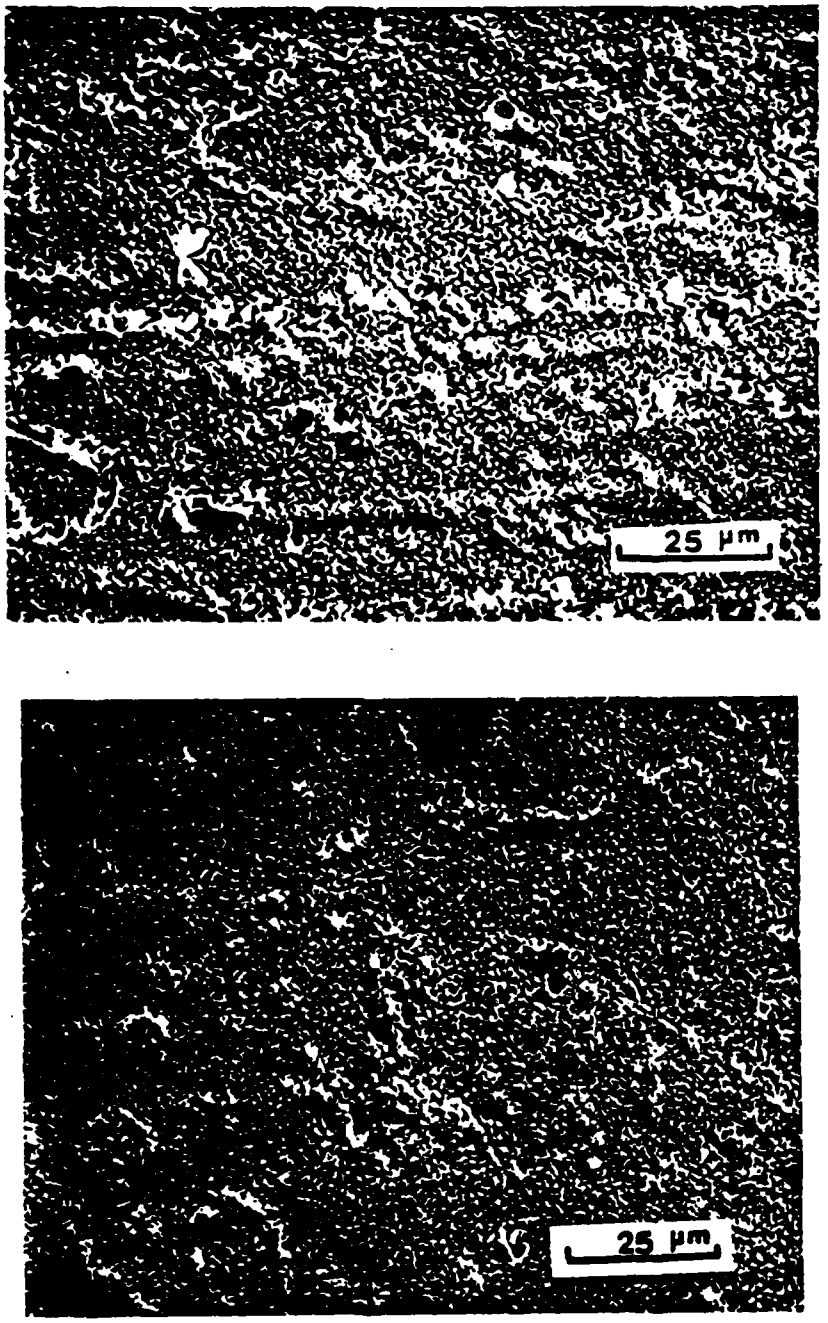

Figure 25. Scanning micrographs of alloy surfaces exposed upon pulling oxide scales from NiCrAl-0.2Y (upper) and NiCrAl-0.3Y (lower) after 48 hours of oxidation in air at 1100°C. Fewer yttrium-rich particles are evident on the NiCrAl-0.3Y specimen.

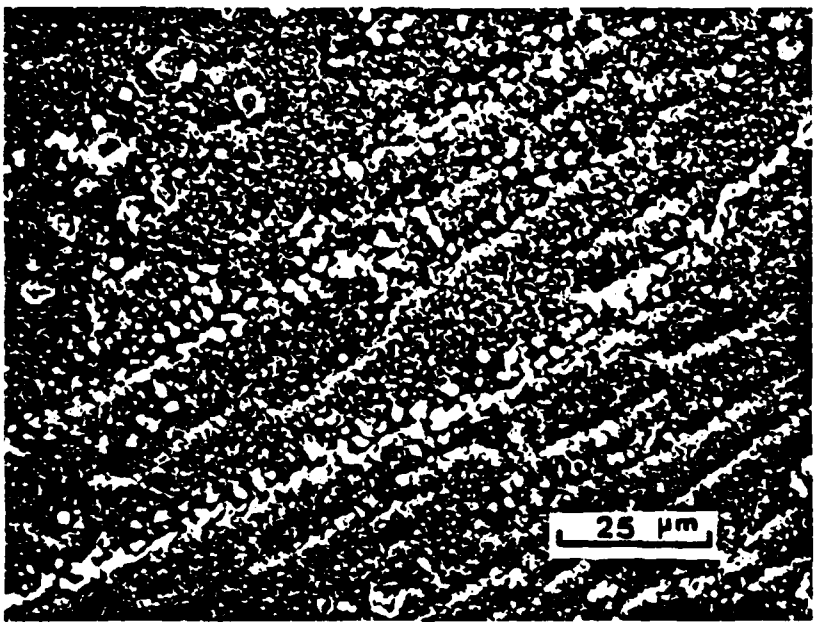

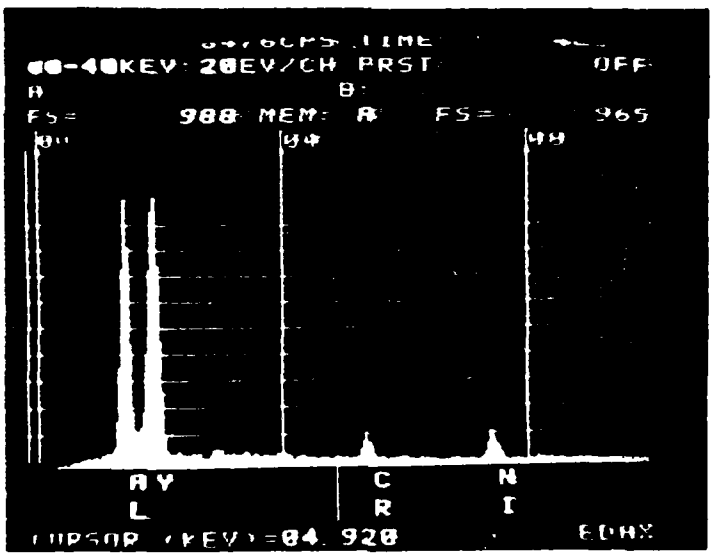

Figure 26. SEM micrograph showing the surface of the alumina scale at the alloy-oxide interface. This scale was removed from the NiCrAl-0.2Y specimen shown in Figure 25. Energy dispersive x-ray analysis showed that the particles which are evident in the scanning micrograph were yttrium rich.


FILM